Supporting Information

Substituent- and temperature-controllable NHC-derived zwitterionic catalyst enables CO$_2$ upgrading for high-efficiency construction of formamides and benzimidazoles

Zhaozhuo Yu, Zhengyi Li, Lilong Zhang, Kaixun Zhu, Hongguo Wu, Hu Li[*], Song Yang[*]

State Key Laboratory Breeding Base of Green Pesticide & Agricultural Bioengineering, Key Laboratory of Green Pesticide & Agricultural Bioengineering, Ministry of Education, State-Local Joint Laboratory for Comprehensive Utilization of Biomass, Center for R&D of Fine Chemicals, Guizhou University, Guiyang, Guizhou 550025, China.

* Corresponding authors.

E-mails: hli13@gzu.edu.cn (HL); jhzx.msm@gmail.com (SY)

Experimental details

The synthesis of Catalysts

The catalysts **1a-1f** were synthesized as follows: The mixture of the corresponding precursor, 4.5 mL dimethyl carbonate, and 10 mL methanol were placed into the Teflon-lined, stainless steel autoclave and then was heated to 110-140 ℃ for 26-48 h. The detailed information about the synthesis of **1a-1f** is shown in Table S1.

Table S1. The particular information about the synthesis of catalysts **1a-1f**

Entry	Catalyst	Precursor	M $_{Pre}{}^{a}$	Time (h)	Temp. (℃)
1	**1a**	1-Methylimidazole	1.98 g	36	110
2	**1b**	1-Methylbenzimidazole	3.30 g	48	140
3	**1c**	1-Propylimidazole	2.66 g	36	110
4	**1d**	1,4-Dimethylimidazole	2.32 g	36	110
5	**1e**	1-Acetylimidazole	2.75 g	48	140
6	**1f**	5-Chloro-1-methylimidazole	2.91 g	48	140

^{a} The weight of the corresponding precursor.

The purification of catalysts

First, the solvent was removed from the resulting reaction mixture by reduced-pressure distillation. Then, for catalyst **1c**, the obtained liquid was washed with acetone six times (6×15 mL) and ether two times (2×10 mL). For the catalysts **1a**, **1b**, **1e**, **1d**, and **1f**, the obtained solids were washed with dichloromethane (15 mL) three times, acetone (15 mL) three times, and ether (10 mL) two times respectively. Finally, all imidazolium-CO_2 adducts were dried under vacuum at room temperature.

A typical procedure for the imidazolium-CO_2 adducts catalyzed the construction of C-N bond for the synthesis of formamide derivatives and benzimidazole-based compounds from benzylamine and *o*-phenylenediamine

The model procedure is detailed for the transformation of amine to formamide or

benzylamine using imidazolium-CO_2 adduct as catalyst (5 mol%) and phenylsilane (0.42 mmol for *N*-formylation,1mmol for cyclization) as silane. A 25 mL reaction tube equipped with a magnetic stir bar and 2 mm glass stopcock was charged with imidazolium-CO_2 adduct at first. Then, the reaction tube was degassed and exposed to carbon dioxide (pressure = 1 bar) and a reaction mixture including 2 mL CH_3CN (or dimethylformamide in cyclization reaction), amine (0.25 mmol), and phenylsilane was injected into the reaction tube. The flask was connected with a CO_2 balloon and stirred for 24 h.

The dissolution test of imidazolium-CO_2 adducts

A 25 mL reaction tube was charged with CH_3CN (2 mL), imidazolium-CO_2 (40 mg). Then, the mixture was degassed and exposed to N_2 (pressure=1 bar). The mixture was stood at room temperature for 24 h. Ensuring the stable existence of imidazolium-CO_2 adducts in CH_3CN, the reaction tube was heated to 80 ℃ for 50 min. Then, until the reaction tube was cooled to room temperature, the reaction mixture was stirred for 24 h under N_2 (or CO_2). Finally, the residual was filtered out through a high-speed centrifuge (10000 rpm, 5 min) and weighed.

The recycling of catalysts and purification of production

The investigation of the catalytic activity for the recycled catalyst was processed as the typical procedure and the reaction condition was optimized (25 ℃, 24 h, 5 mol% catalyst, 0.25 mmol amine). After the completion of the *N*-formylation reaction, the solid siloxane was removed from the reaction mixture by a high-speed centrifuge (10000 rpm, 5 min). Then, the solvent CH_3CN was removed by reduced pressure distillation. The residual was added to diethyl ether (5 mL). Until the residual cannot dissolve into the ether continually, the solid in the solution was filtered out by a high-speed centrifuge (10000 rpm, 5 min) and dried in a vacuum for 24 h, which is the recycled imidazolium-CO_2. The ether in the residual liquid was removed by a high-speed centrifuge (10000 rpm, 5 min) and the residual solid was the purified product.

The in-situ FTIR analysis for NHC-CO$_2$

The in-situ FTIR spectra were carried out using a Thermo Fisher Nicolet iS5 FT-IR spectrometer. The temperature was controlled with a thermocouple. The background spectra were recorded at first. Then, NHC-CO$_2$ was loaded into the in-situ FTIR cell and flushed with N$_2$ (100 mL min^{-1}) for 30 min and the temperature of the system was raised at a rate of 1 ℃ min^{-1} from 25 ℃ to 80 ℃. The process was repeated twice under the same conditions. The spectra were recorded every minute.

The analysis of the sample

The concentrations of the product obtained from the *N*-formylation and cyclization reaction were determined by using a GC instrument equipped with an HP-5 chromatographic column (30 m × 0.320 mm × 0.25 μm) and an FID, using naphthalene as an internal standard referring to the standard curves (R^2 >0.999) obtained with commercial specimens. The formula for calculating the yield and conversion are as follows:

$$\text{Conversion (\%)} = (1 - \frac{\text{mole of residual substrate}}{\text{mole of initial substrate}})\times100\%$$

$$\text{Yield (\%)} = \frac{\text{mole of product}}{\text{mole of initial substrate}} \times100\%$$

Computational details

All optimized structure and energy calculations were performed with density functional theory (DFT) using the M06-2x functional implemented in the Gaussian 09 Revision D.01 software at ambient pressure (1 atm) and room temperature. The 6-311G(d,p) all-electron basis was set for main group elements in this study.

Table S2. Computational data for chemical property assessment of catalysts **1a-1f**

Catalyst	$P_O{}^a$	$P_C{}^b$	$L_{C\text{-}C}{}^{,c}$

Catalyst **1a**	-0.709	0.096	1.588
Catalyst **1b**	-0.703	0.097	1.623
Catalyst **1c**	-0.705	0.094	1.589
Catalyst **1d**	-0.704	0.094	1.602
Catalyst **1e**	-0.677	0.123	1.579
Catalyst **1f**	-0.709	0.111	1.588

[a] The charge population of oxygen atom in the carboxyl groups of catalysts **1a-1f**

[b] The charge population of carbon atom between two nitrogen atoms in the NHC, which is separated from catalysts **1a-1f**

[c] The bond Length of C-C bond that connects with the carboxyl and imidazole group.

Table S3. The dissolution and precipitation of catalysts in CH_3CN.

Entry	Catalyst	Residue mass ratio [a]	
		N_2 [b]	CO_2 [c]
1	Catalyst **1a**	36.92%	83.72%
2	Catalyst **1b**	95.87%	96.69%
3	Catalyst **1d**	92.06%	96.47%
4	Catalyst **1e**	0%	10.36%
5	Catalyst **1f**	0%	0%

[a] The mass proportion of precipitate on the total catalyst.

[b] The precipitate produced under N_2 condition (1 atm) at room temperature for 48 h.

[c] The precipitate produced under CO_2 condition (1 atm) at room temperature for 48 h.

Characterization
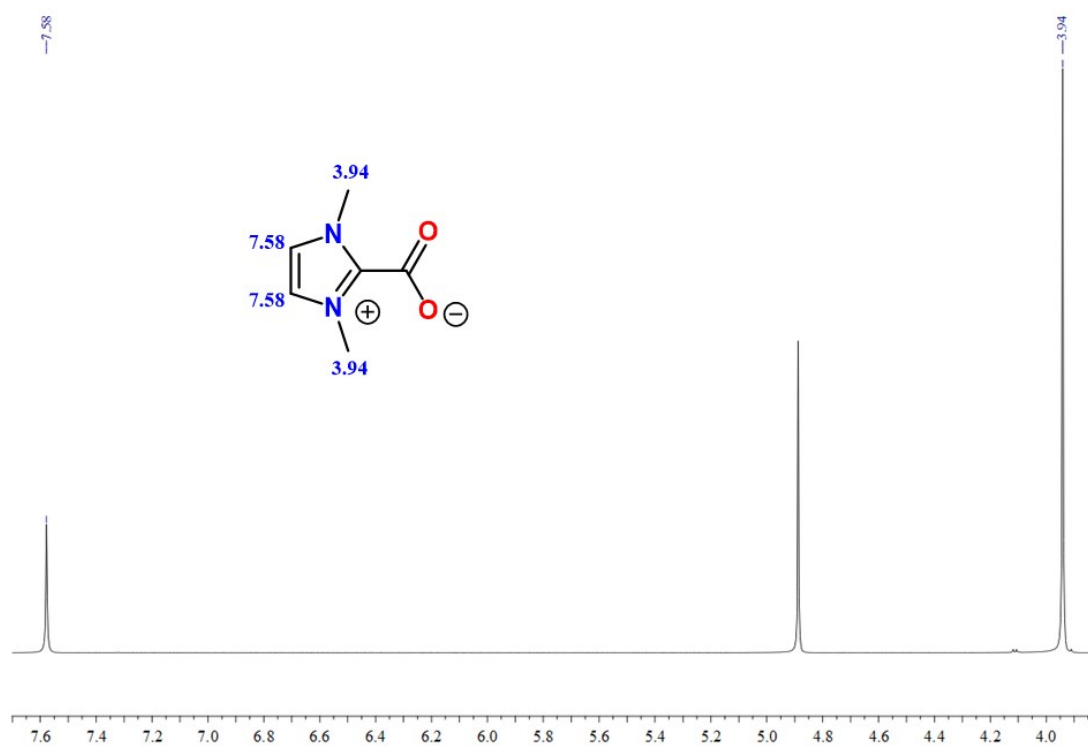
Figure S1. The ^{1}H NMR spectrum (in CD$_3$OD) of 1,3-dimethylbenzimidazolium-2-carboxylate (**1a**).
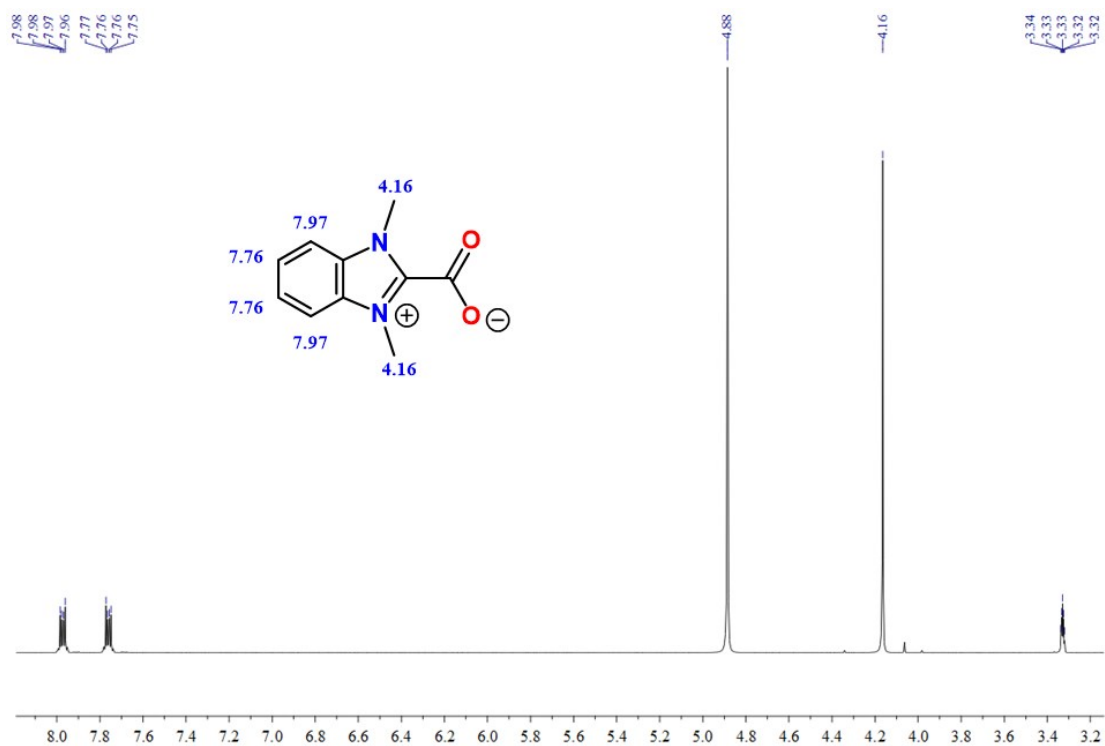
Figure S2. The ^{1}H NMR spectrum (in CD$_3$OD) of 1,3-dimethylbenzimidazolium-2-carboxylate (**1b**).
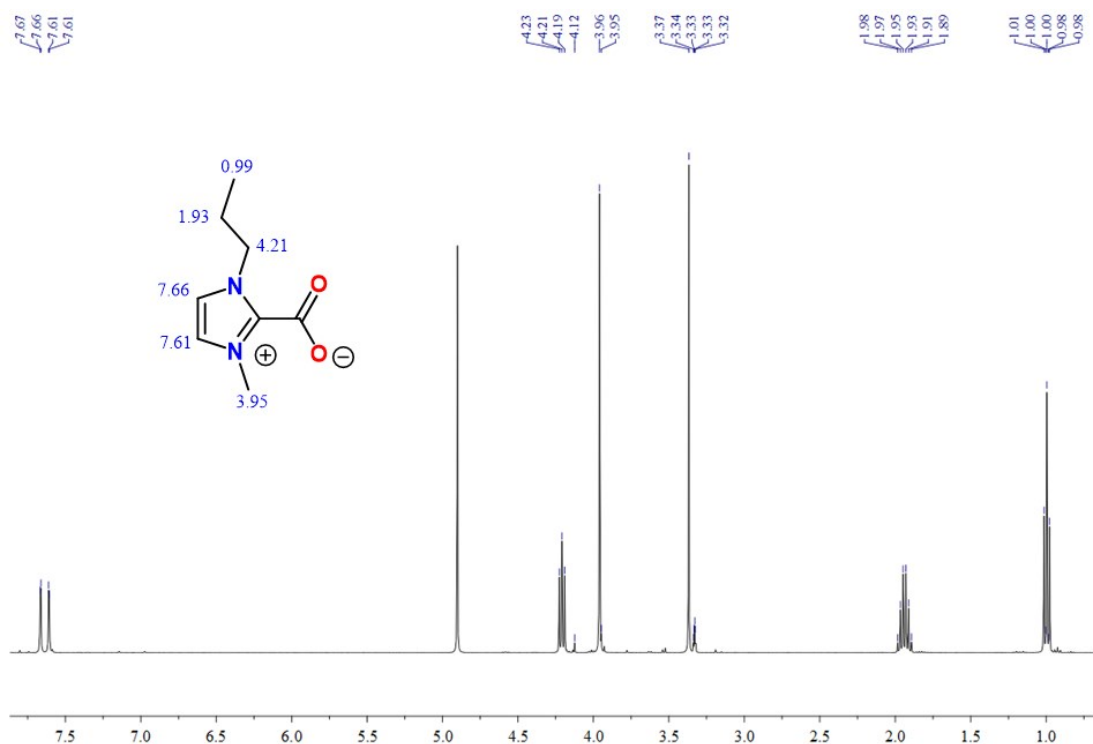
Figure S3. The ^{1}H NMR spectrum (in CD$_3$OD) of 1-propyl-3-methylimidazolium-2-carboxylate (**1c**).
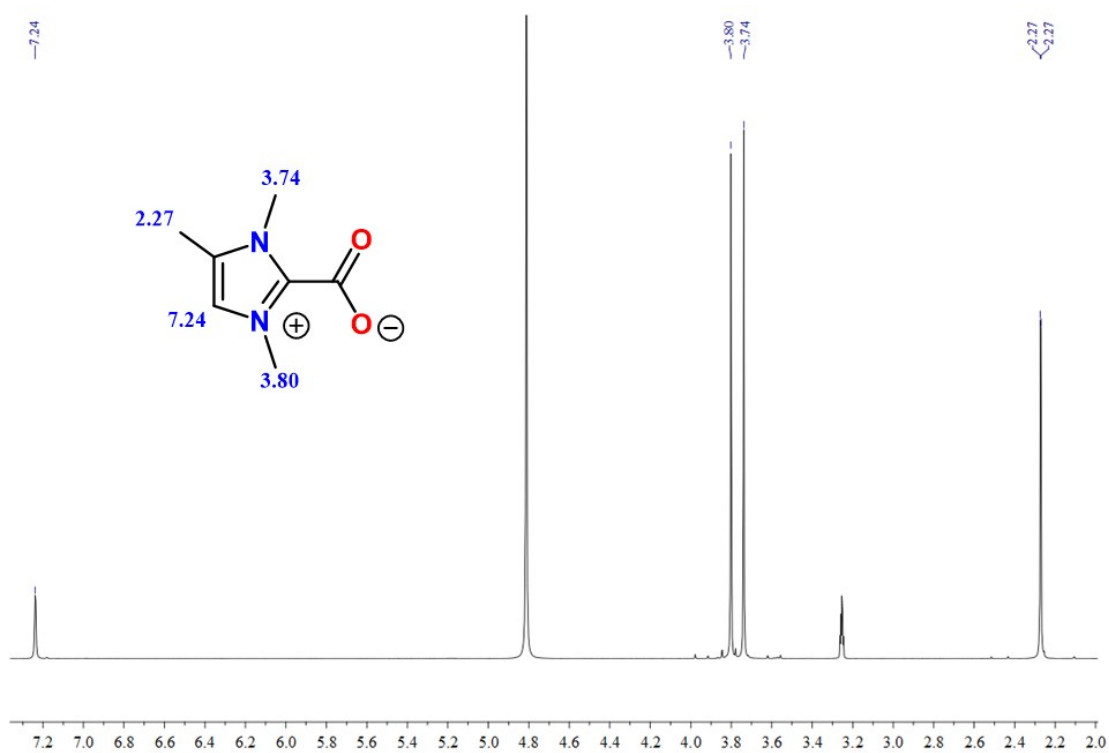
Figure S4. The ^{1}H NMR spectrum (in CD$_3$OD) of 1,3,4-trimethylbenzimidazolium-2-carboxylate (**1d**).
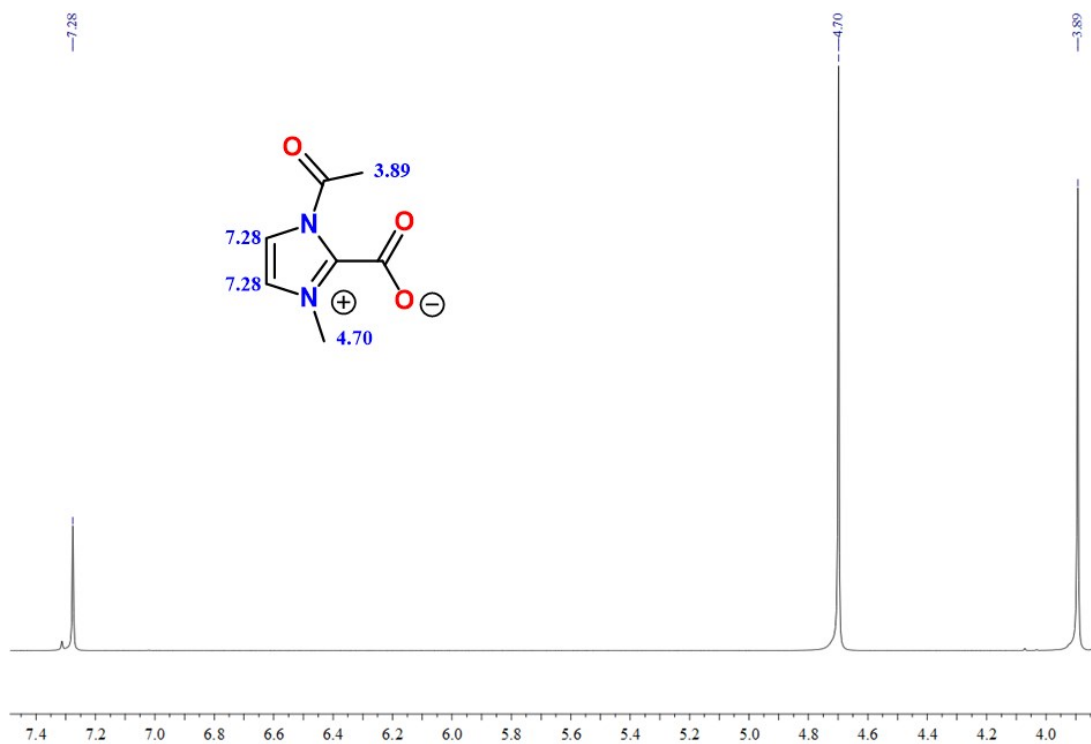
Figure S5. The ^{1}H NMR spectrum (in D$_2$O) of 1-acetyl-3-methylimidazolium-2-carboxylate (**1e**).
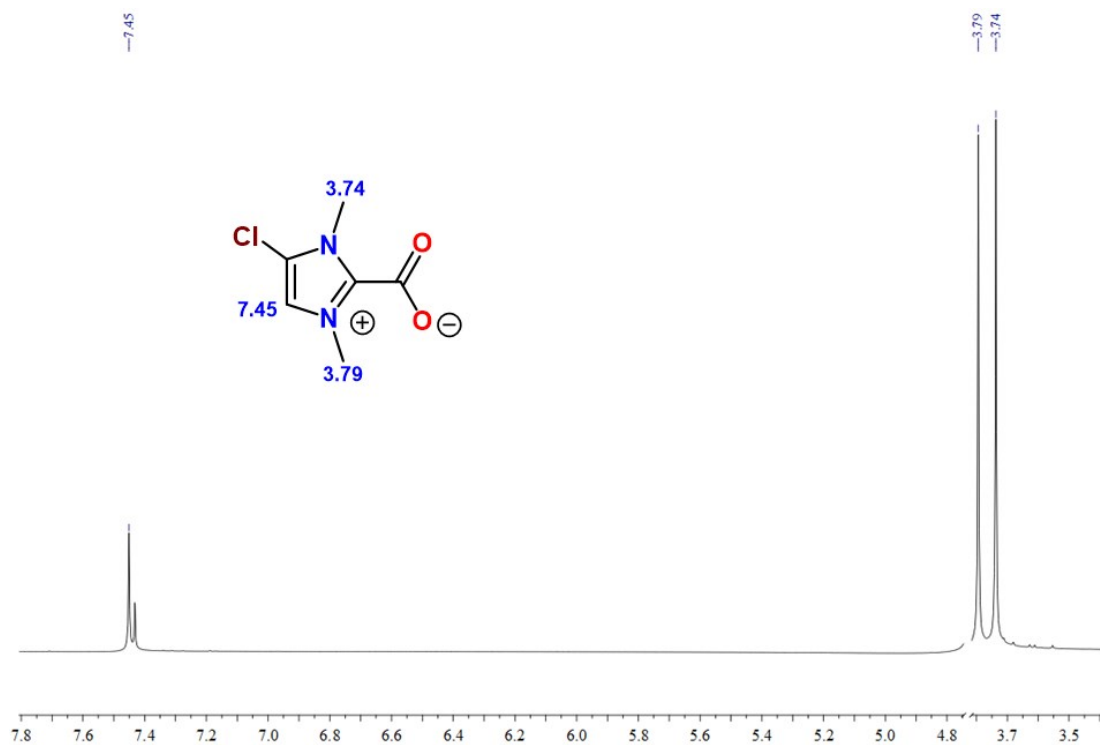
Figure S6. The ^{1}H NMR spectrum (in D$_2$O) of 5-chloro-1,3-dimethylimidazolium-2-carboxylate (**1f**).
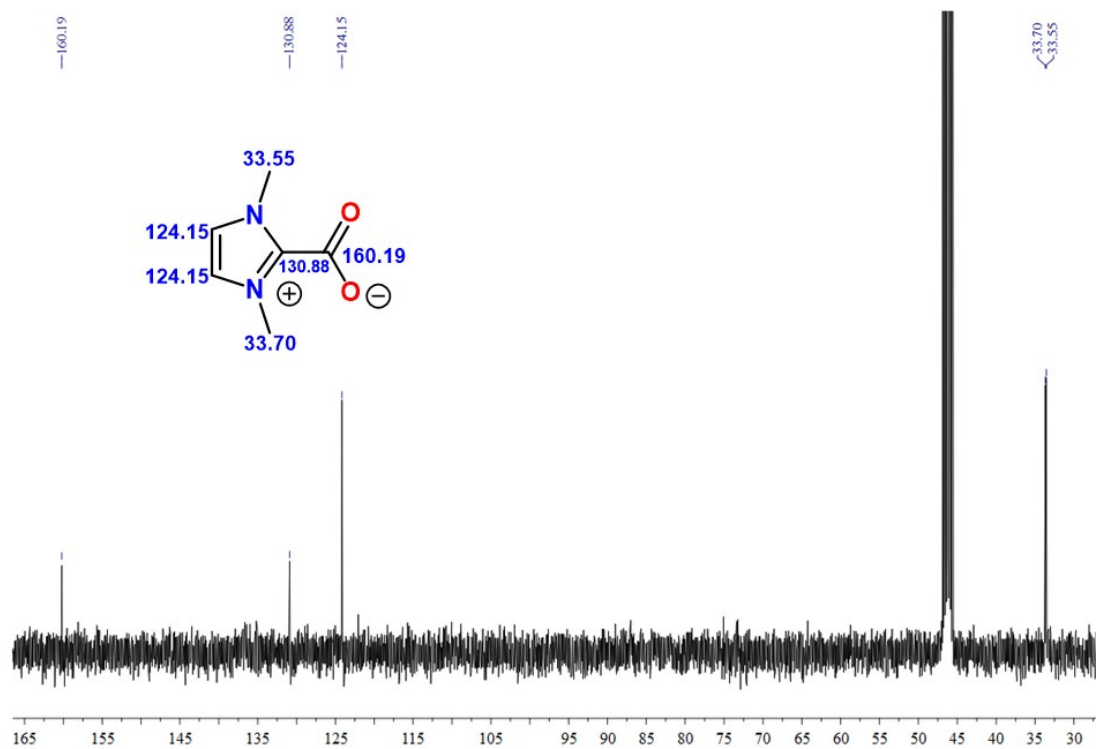
Figure S7. The ^{13}C NMR spectrum (in CD$_3$OD) of 1,3-dimethylbenzimidazolium-2-carboxylate (**1a**).
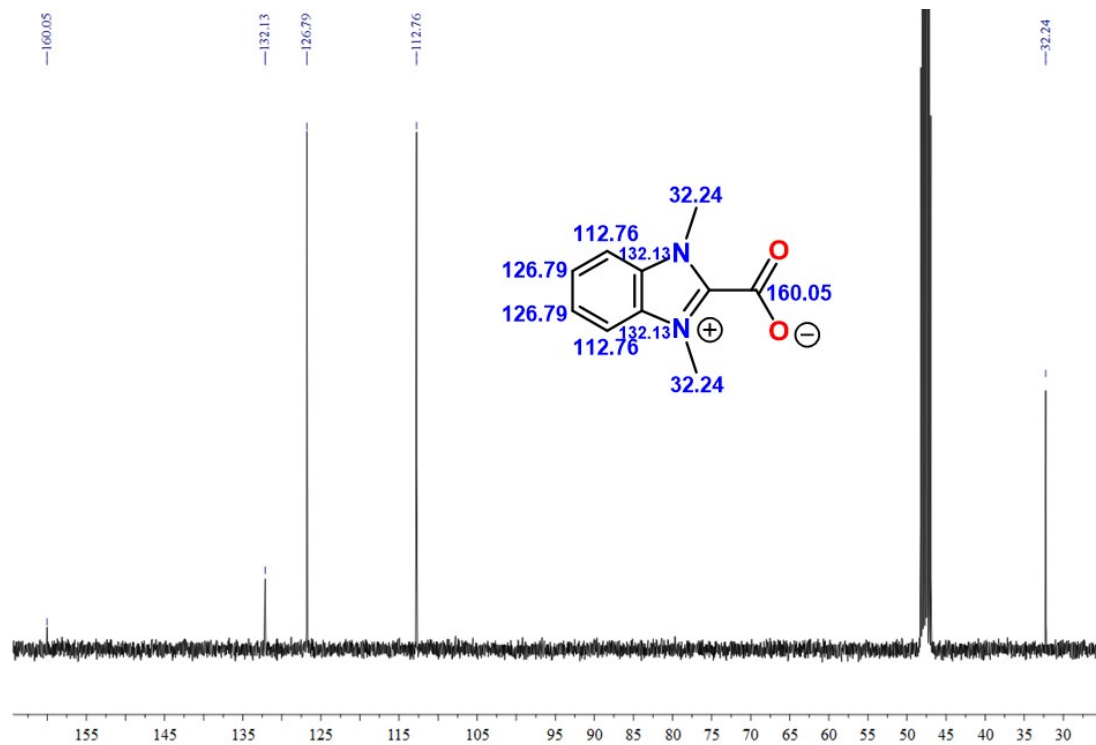
Figure S8. The ^{13}C NMR spectrum (in CD$_3$OD) of 1,3-dimethylbenzimidazolium-2-carboxylate (**1b**).
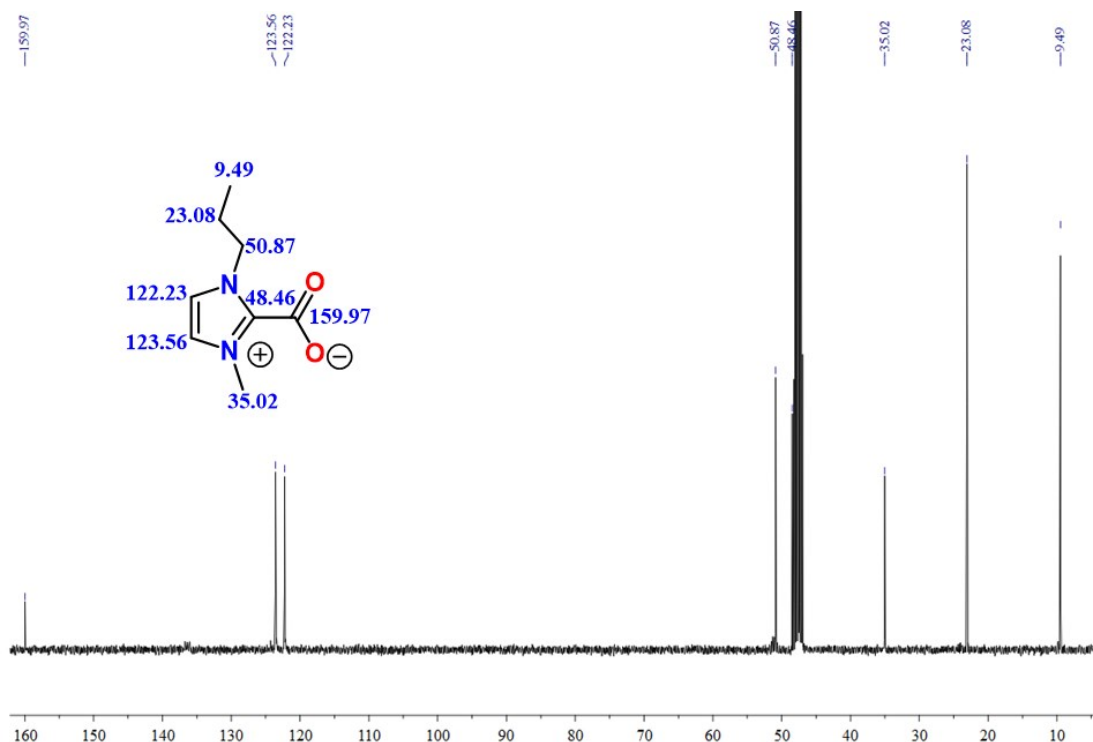
Figure S9. The ^{13}C NMR spectrum (in CD_3OD) of 1-propyl-3-methylimidazolium-2-carboxylate (**1c**).
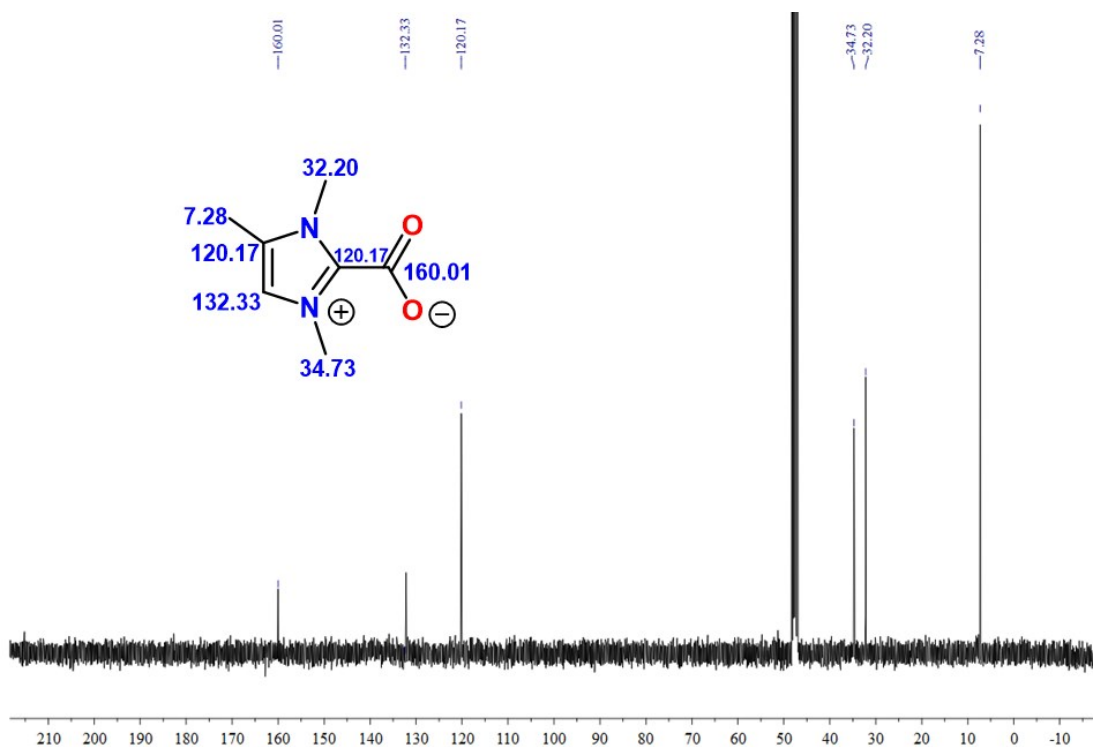
Figure S10. The ^{13}C NMR spectrum (in CD_3OD) of 1,3,4-trimethylbenzimidazolium-2-carboxylate (**1d**).
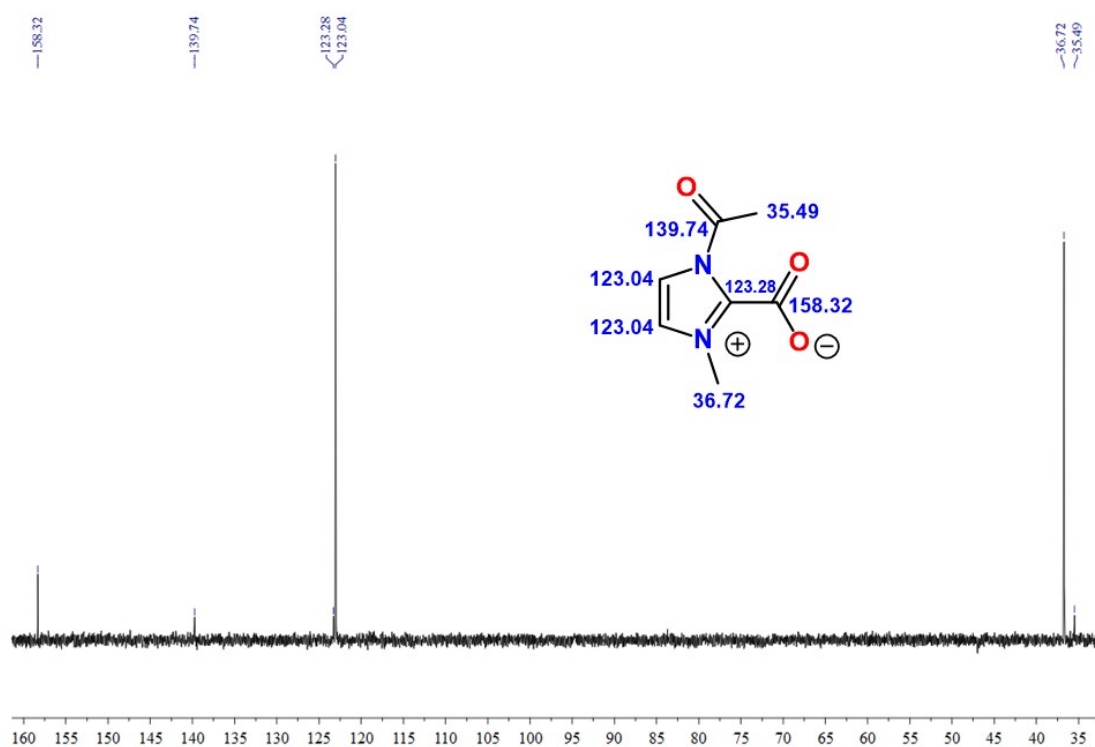
Figure S11. The ^{13}C NMR spectrum (in D$_2$O) of 1-acetyl-3-methylimidazolium-2-carboxylate (**1e**).
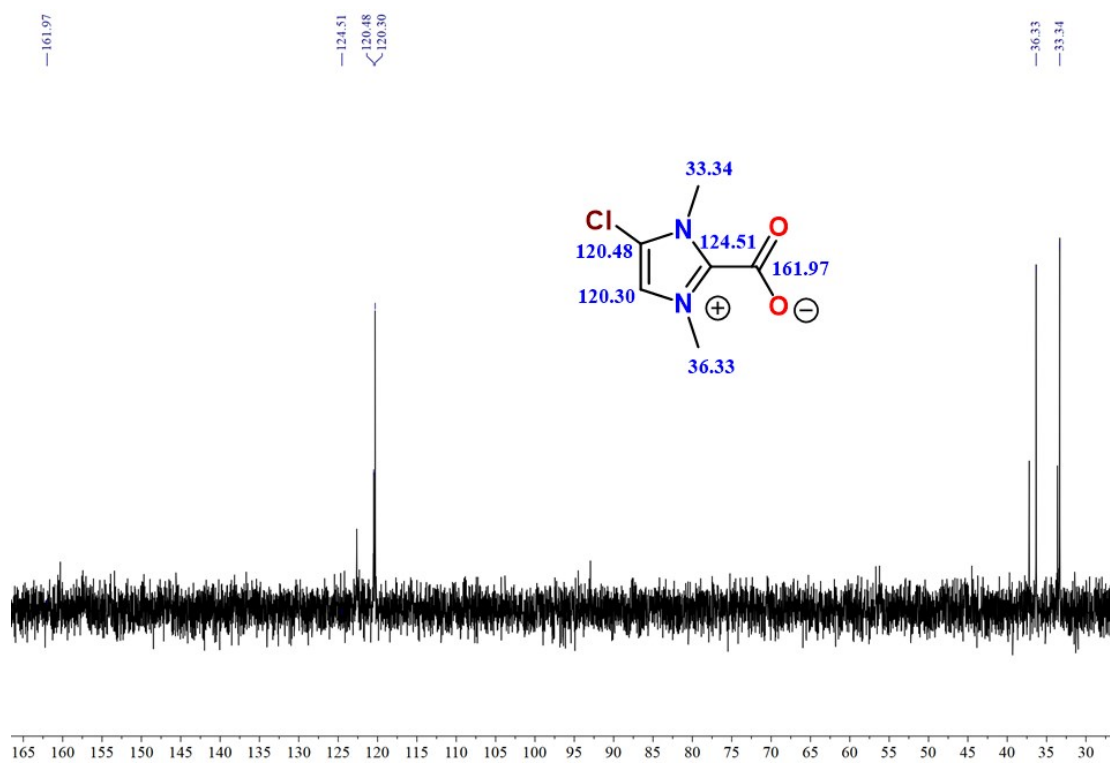
Figure S12. The ^{13}C NMR spectrum (in D$_2$O) of 5-chloro-1,3-dimethylimidazolium-2-carboxylate (**1f**).
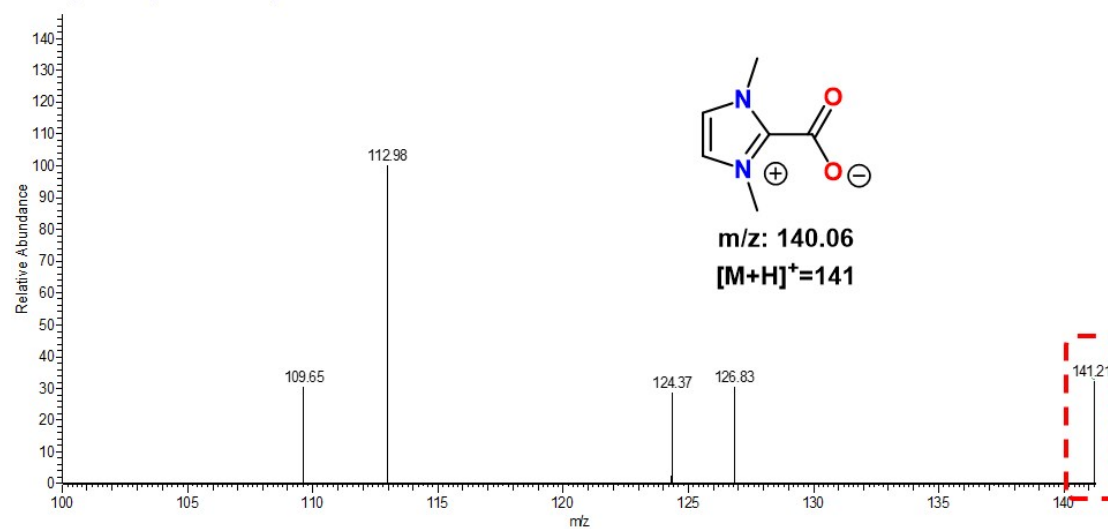
Figure S13. The mass spectrum of 1,3-dimethylbenzimidazolium-2-carboxylate (**1a**).
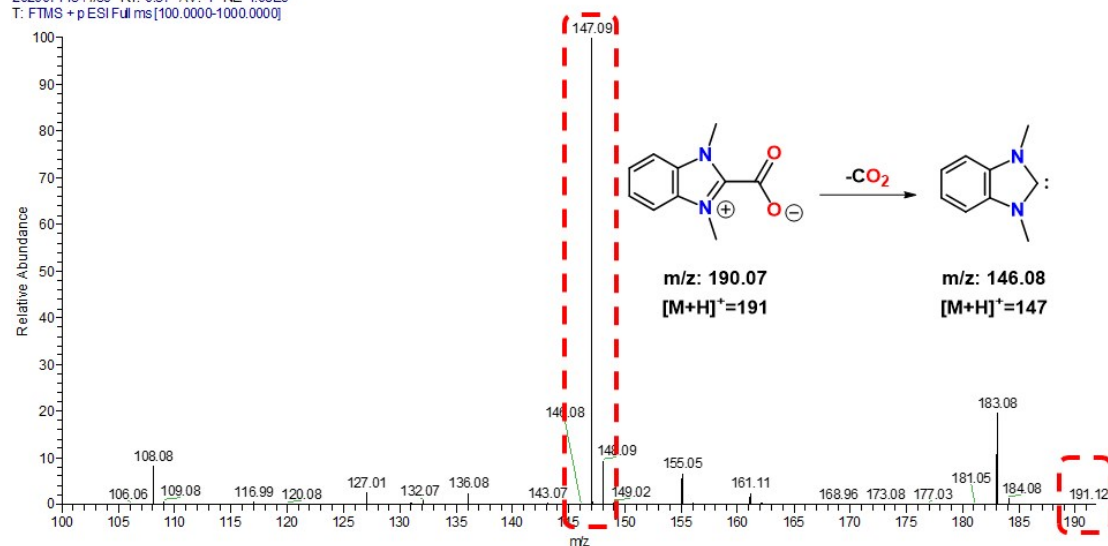
Figure S14. The mass spectrum of 1,3-dimethylbenzimidazolium-2-carboxylate (**1b**).
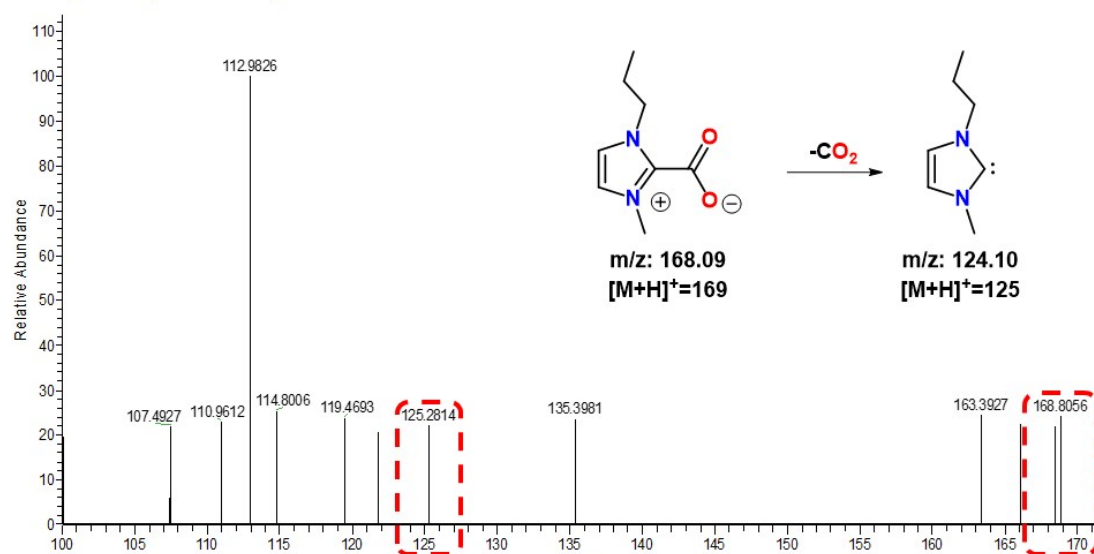
Figure S15. The mass spectrum of 1-propyl-3-methylimidazolium-2-carboxylate (**1c**).
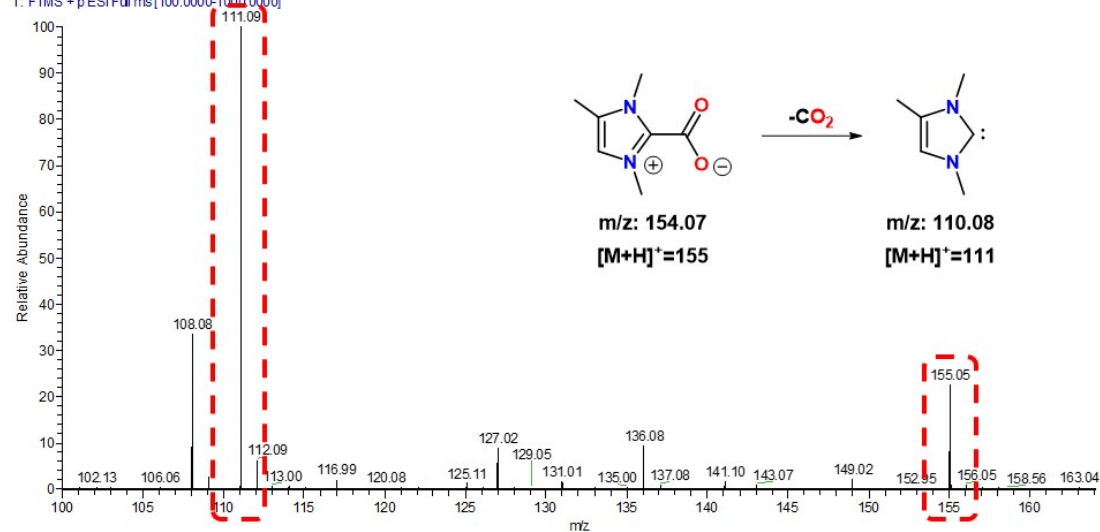
Figure S16. The mass spectrum of 1,3,4-trimethylbenzimidazolium-2-carboxylate (**1d**).
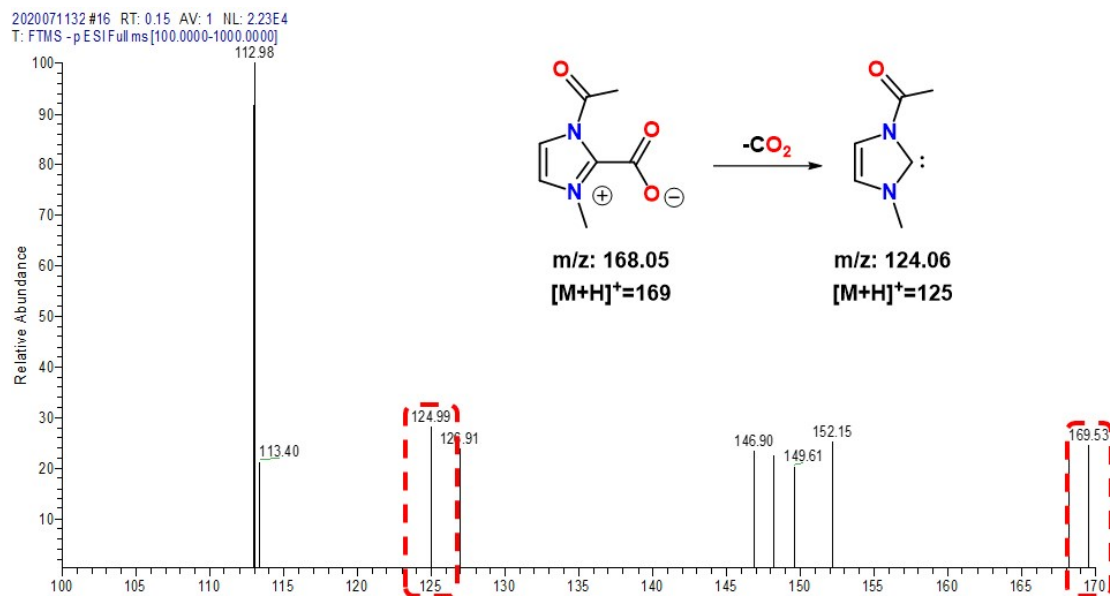
Figure S17. The mass spectrum of 1-acetyl-3-methylimidazolium-2-carboxylate (**1e**).
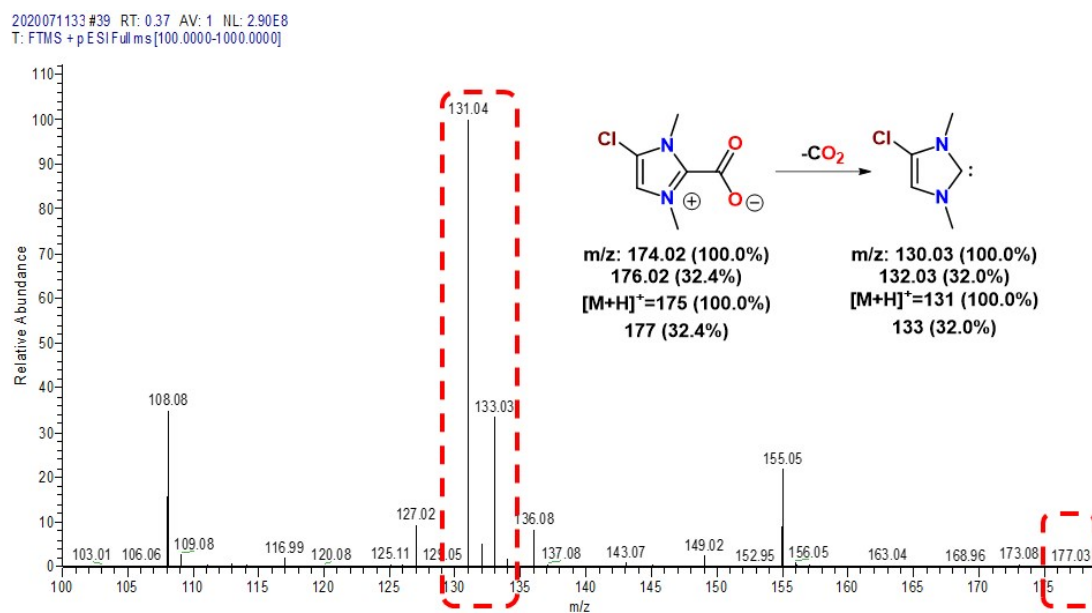
Figure S18. The mass spectrum of 5-chloro-1,3-dimethylimidazolium-2-carboxylate (**1f**).
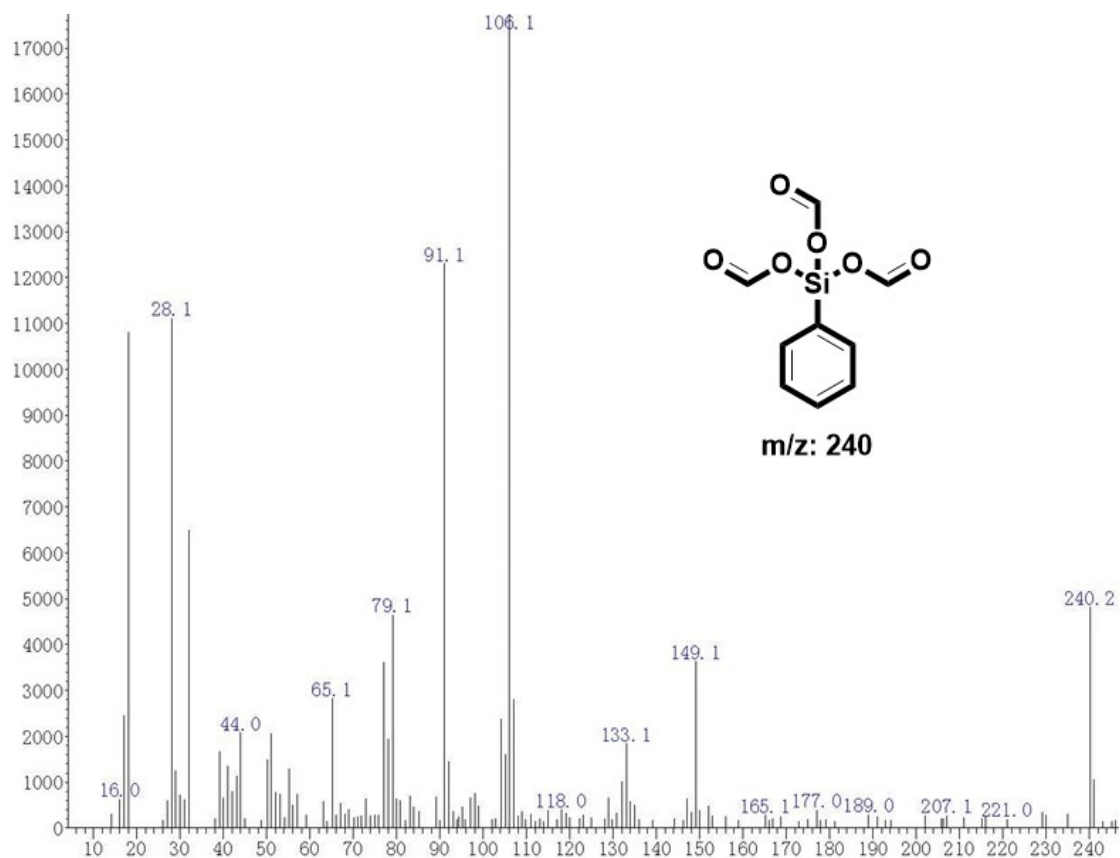
Figure S19. The mass spectrum of phenylsilanetriyl triformate.
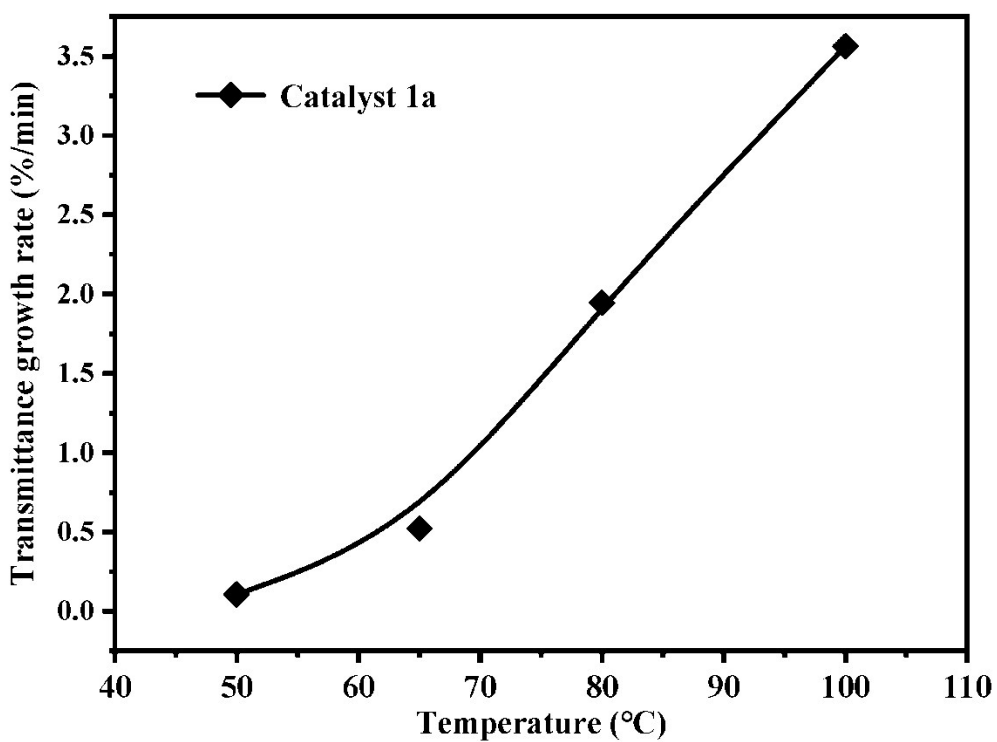
Figure S20. Plots of maximum transmittance growth rate at 1715 cm^{-1} for the

decomposition of **1a** at varying temperature.
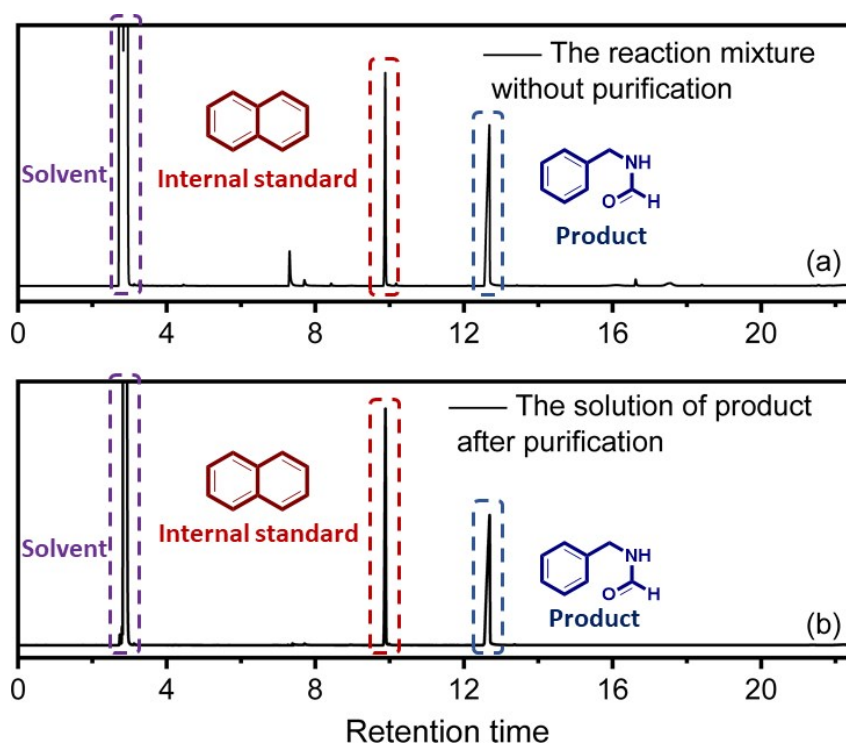
Figure S21. The gas chromatography graphs of reaction mixture (a) before and (b) after purification.
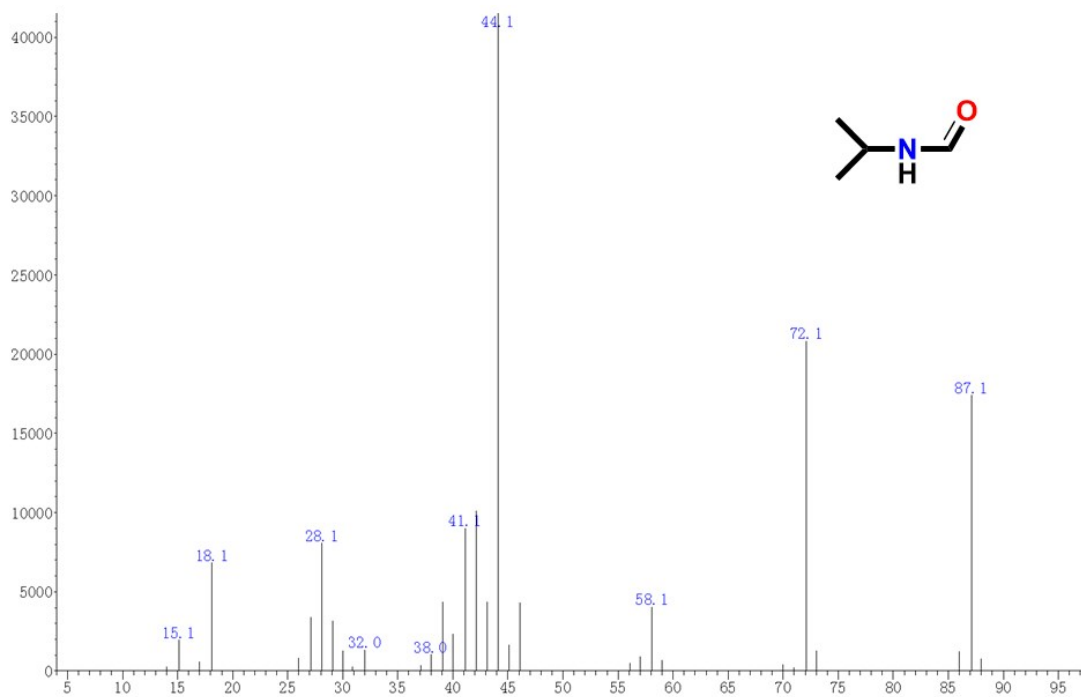
Figure S22. The mass spectrum of **3a**.
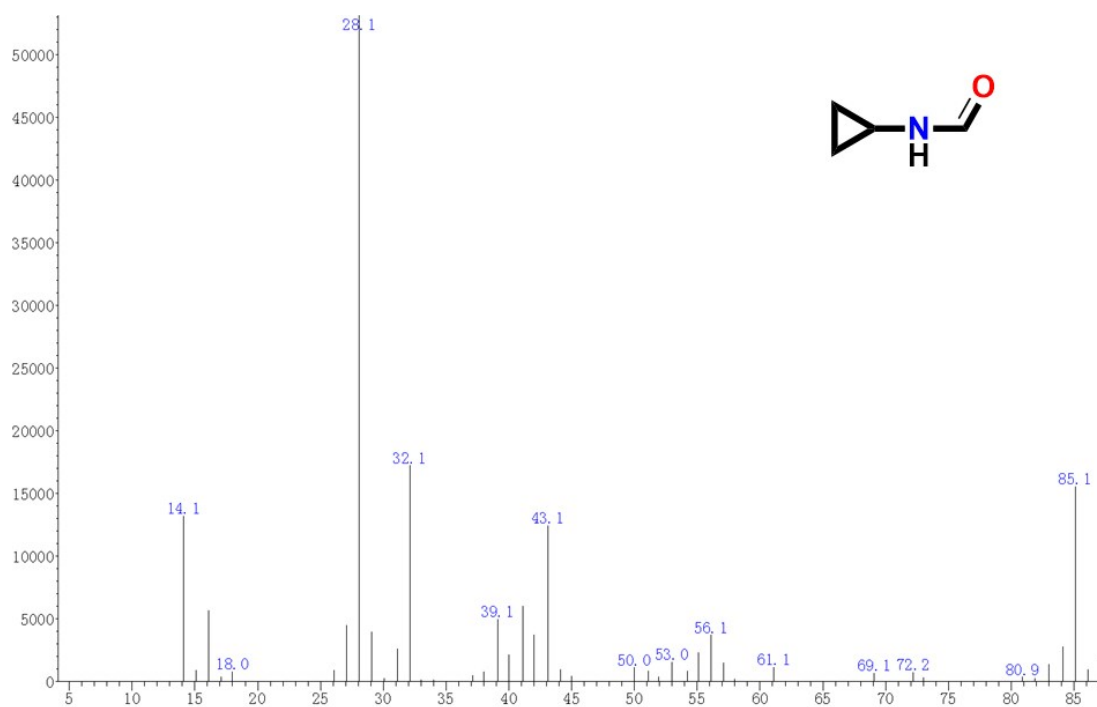
Figure S23. The mass spectrum of **3b**.
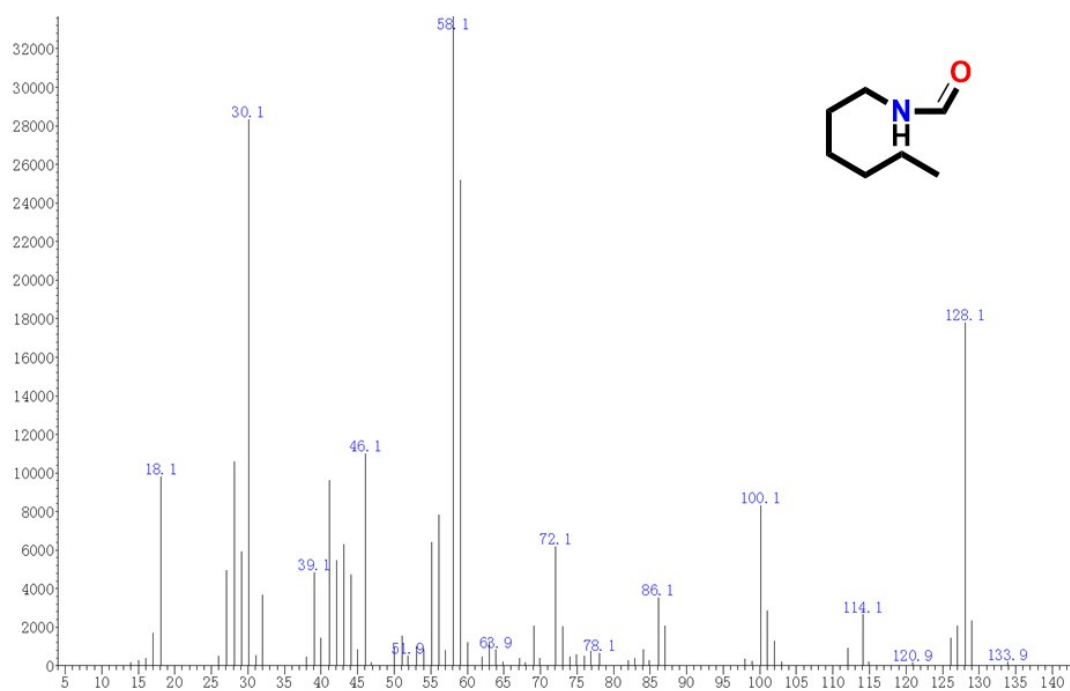
Figure S24. The mass spectrum of **3c**.
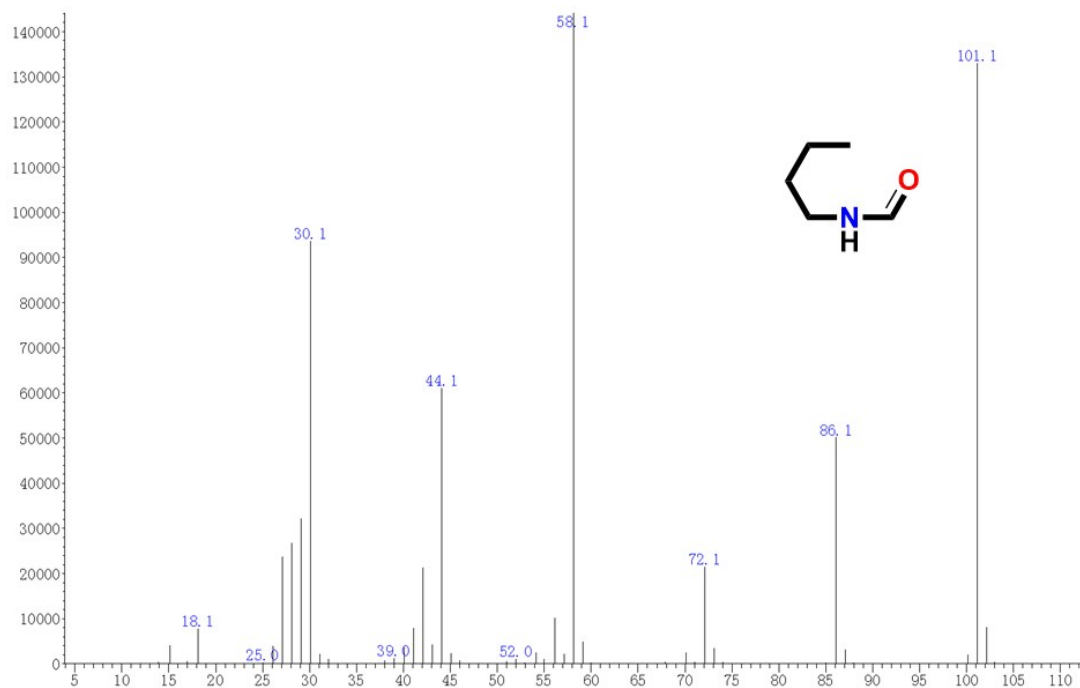
Figure S25. The mass spectrum of **3d**.
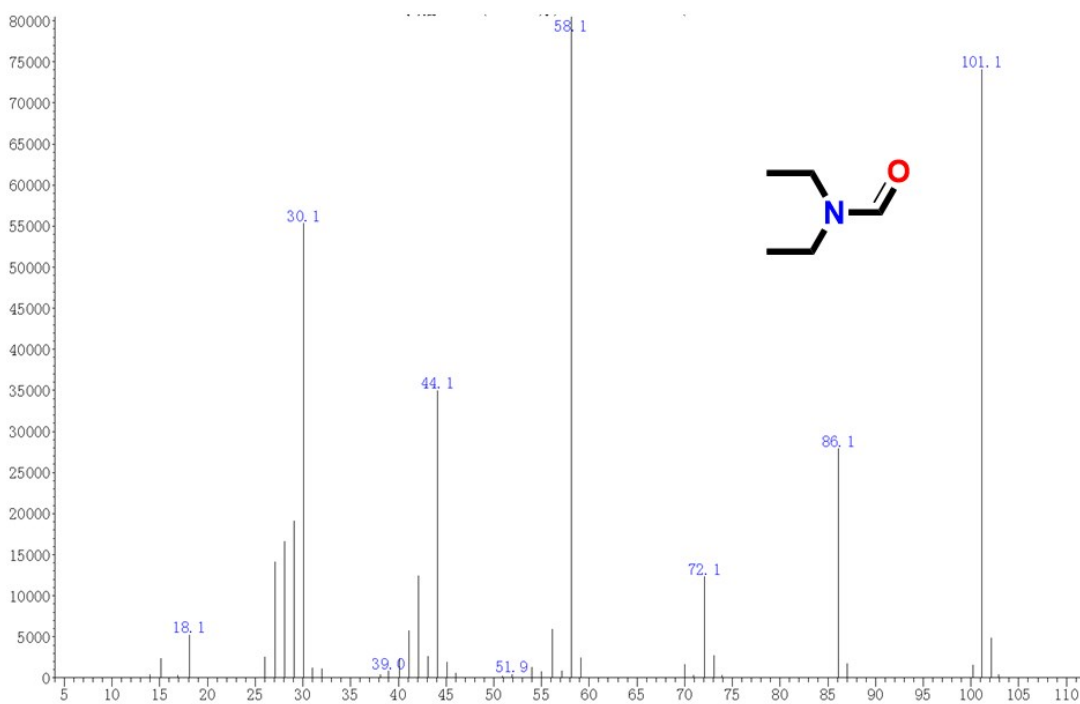
Figure S26. The mass spectrum of **3e**.
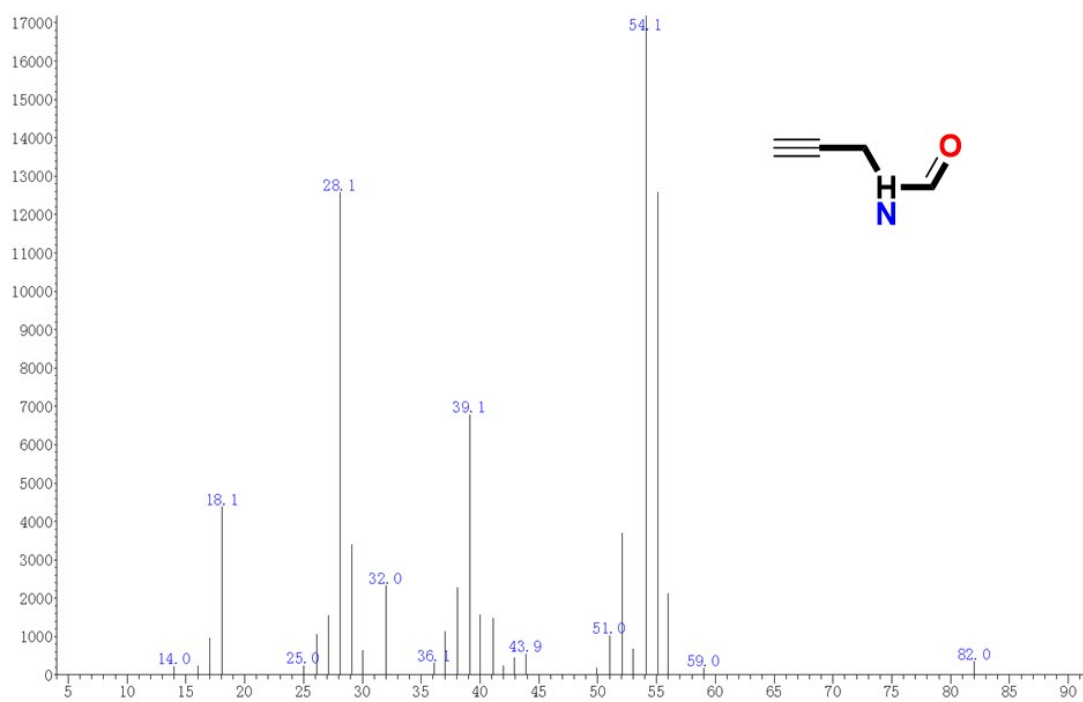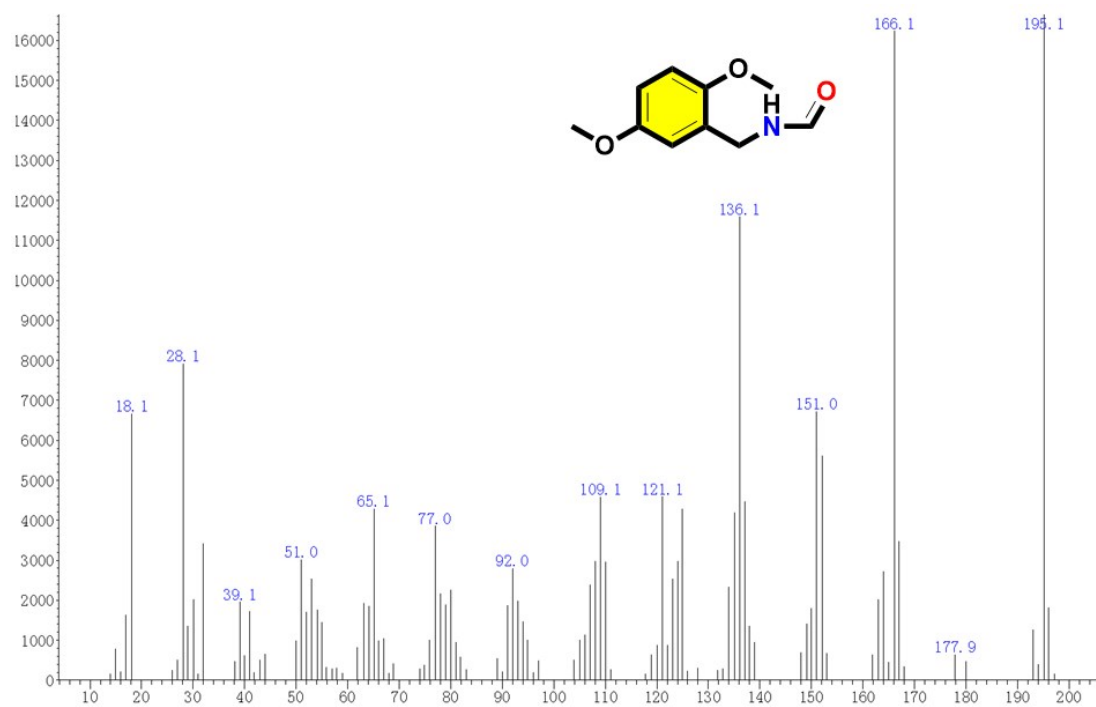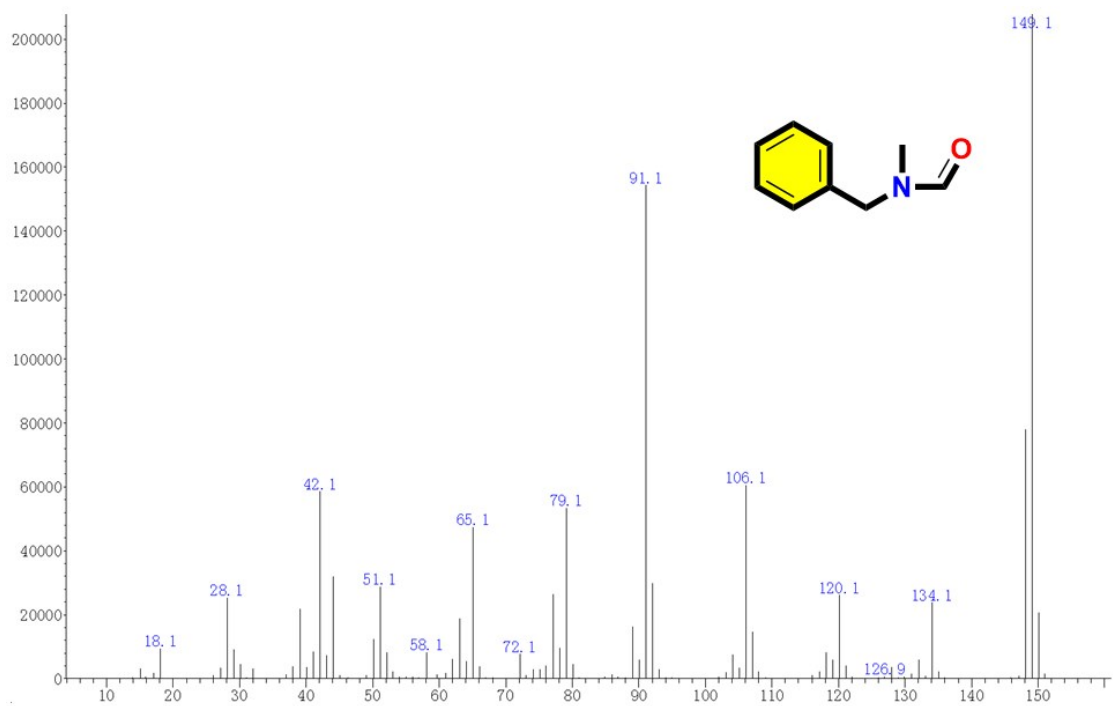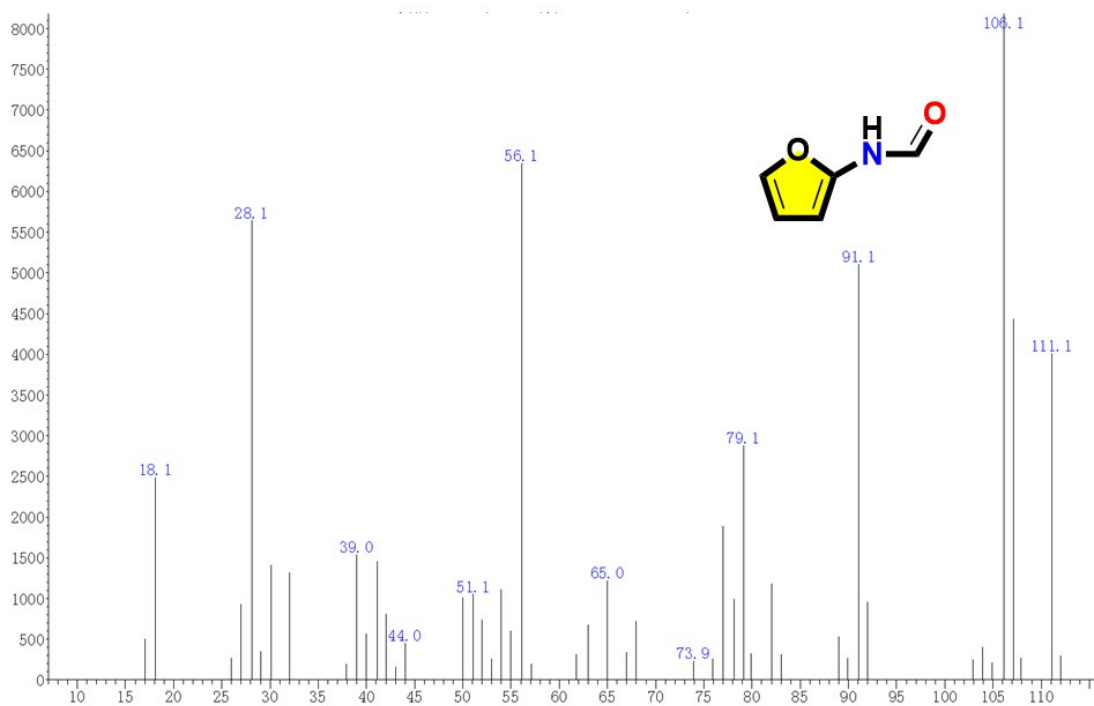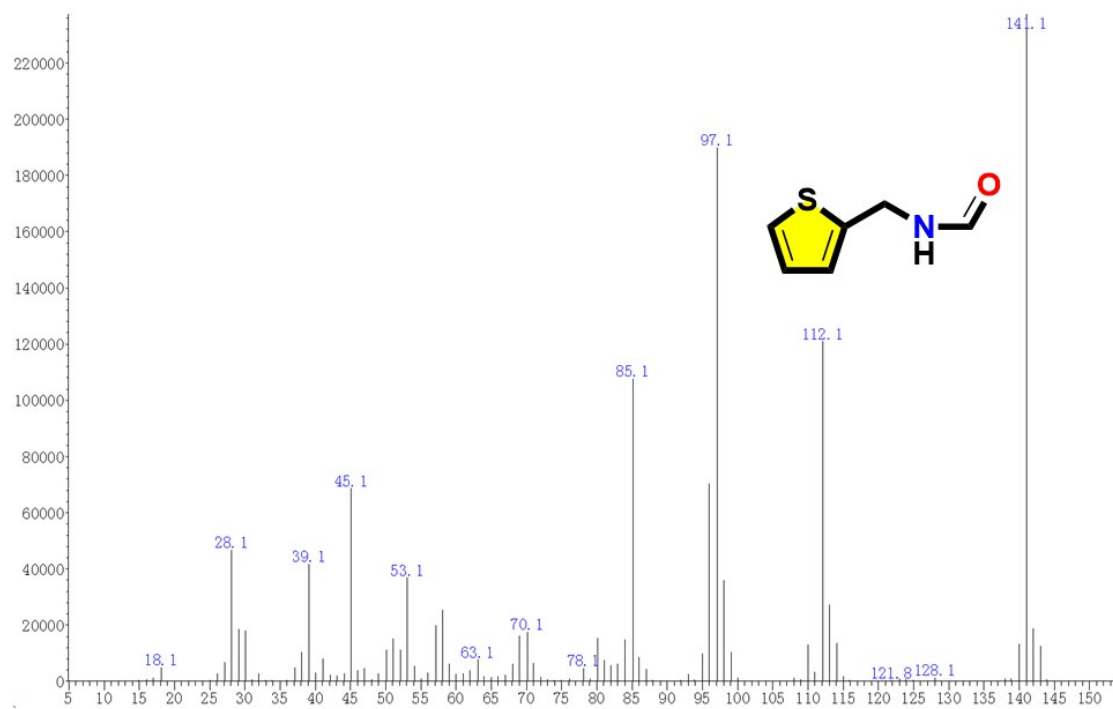
Figure S27. The mass spectrum of **3f**.
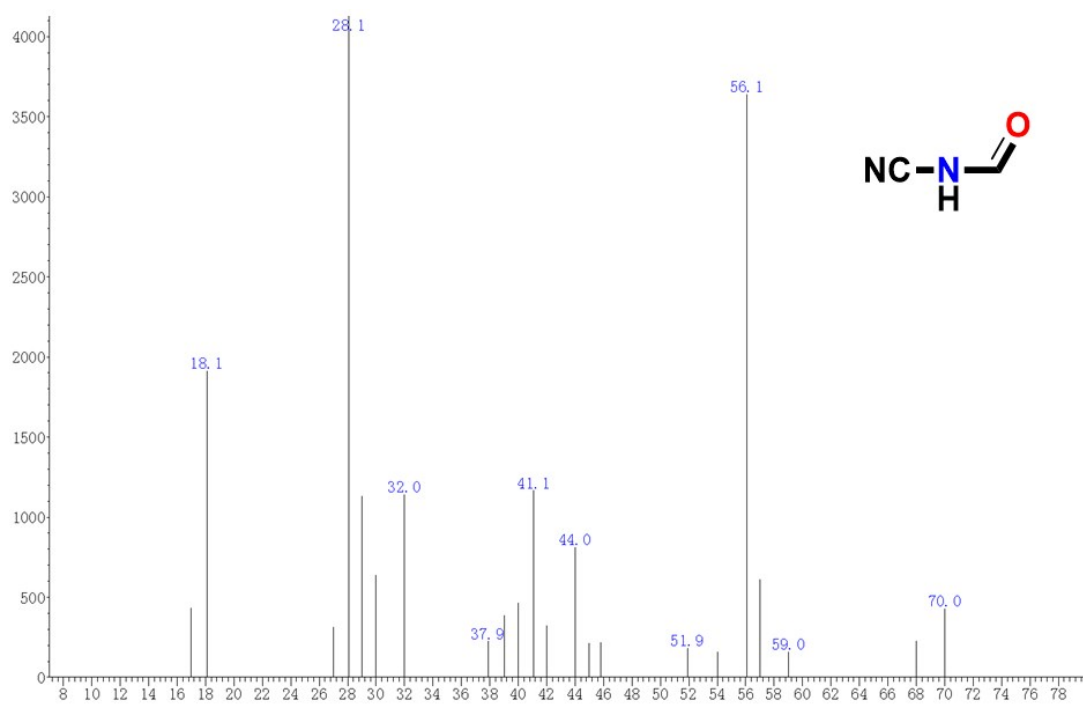
Figure S28. The mass spectrum of **3g**.
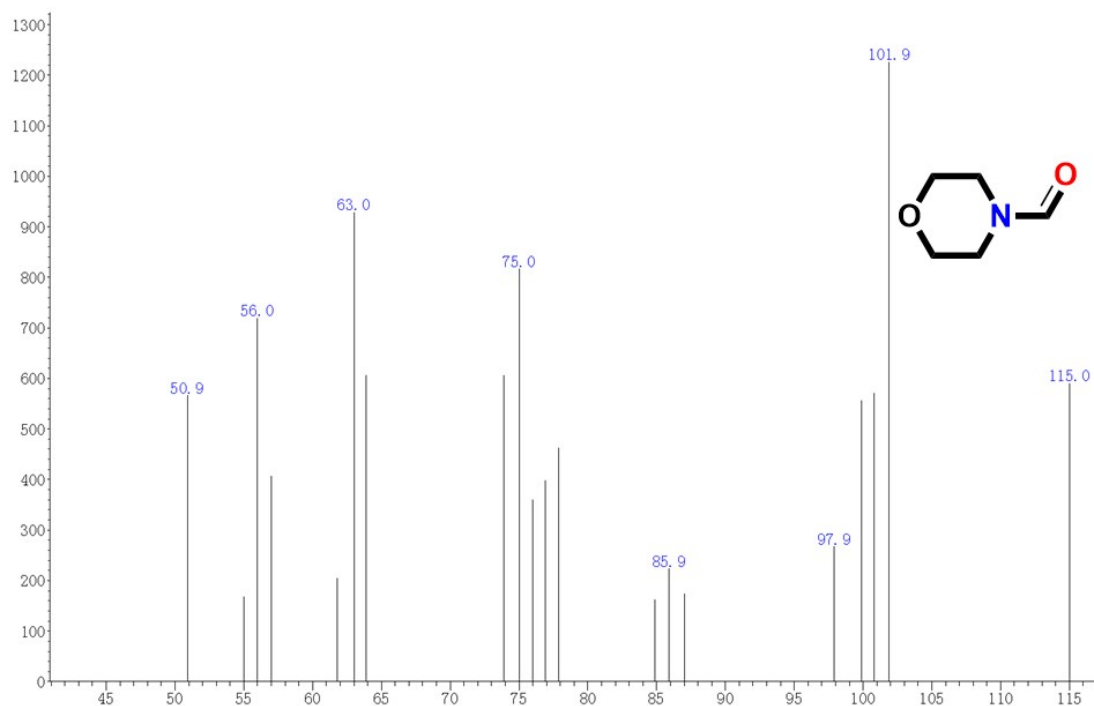
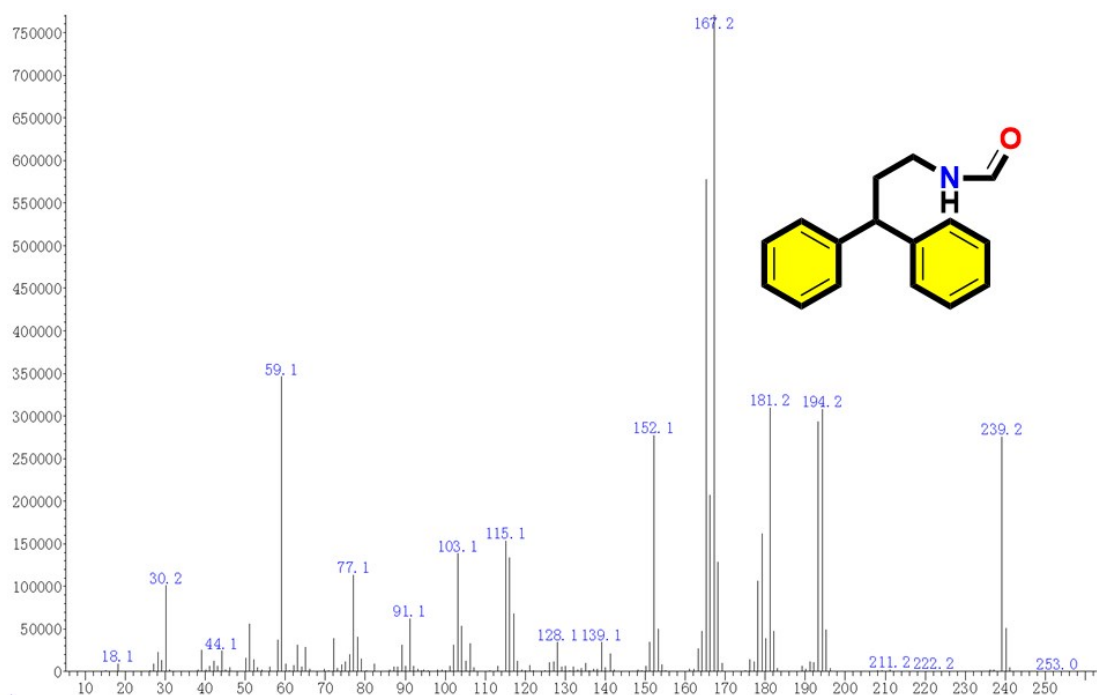**Figure S29.** The mass spectrum of **3h**.
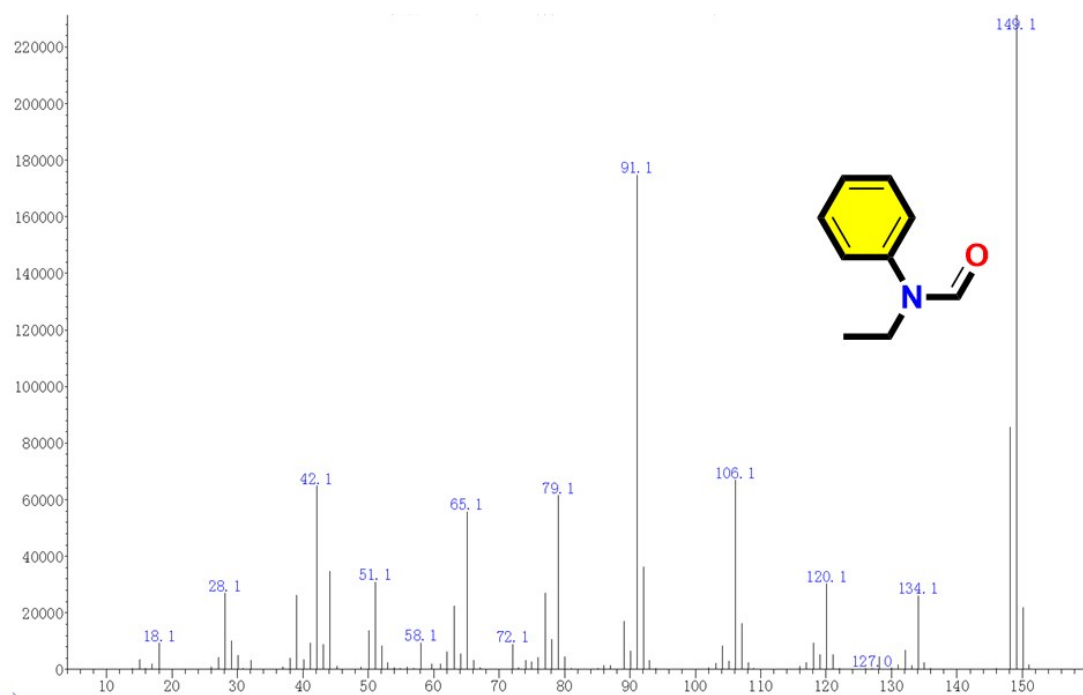
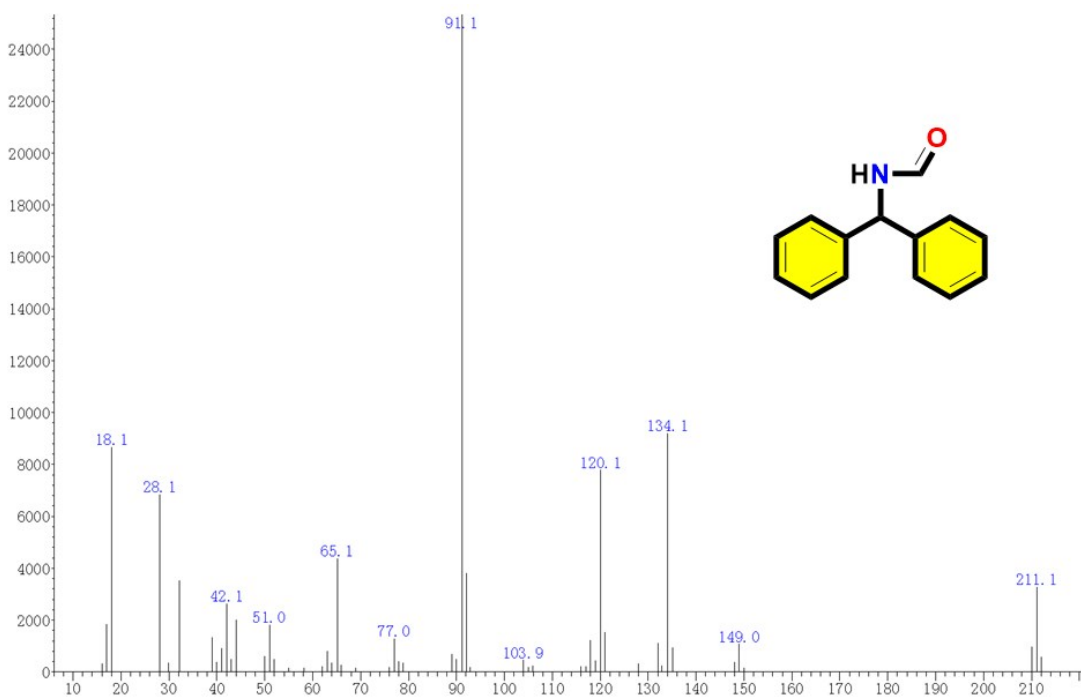**Figure S30.** The mass spectrum of **3i**.
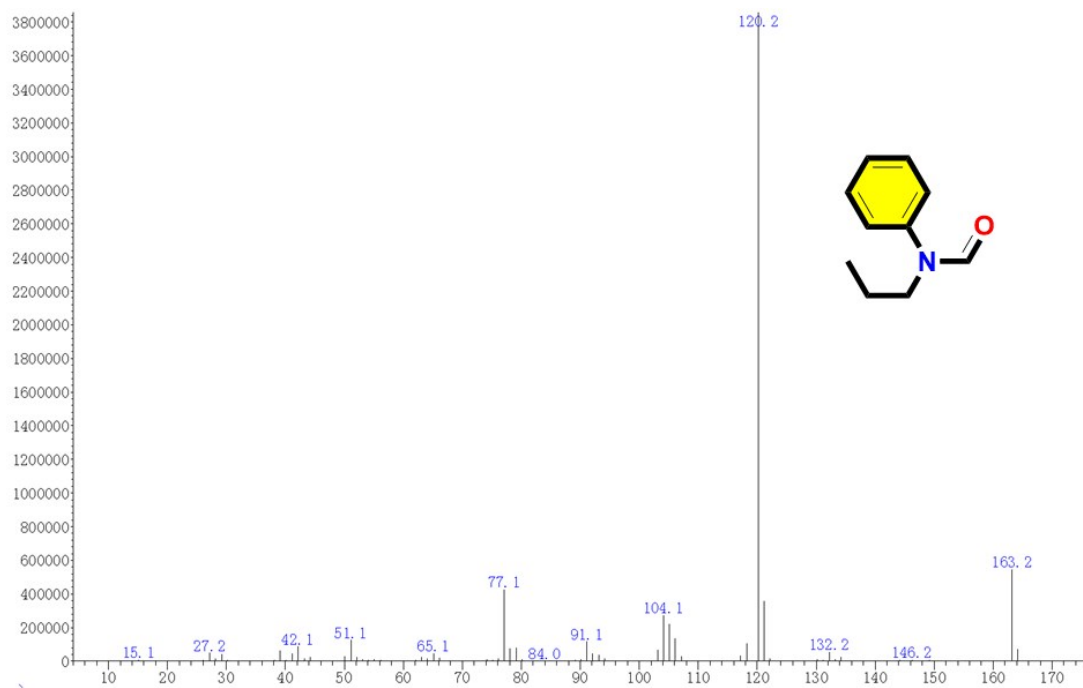
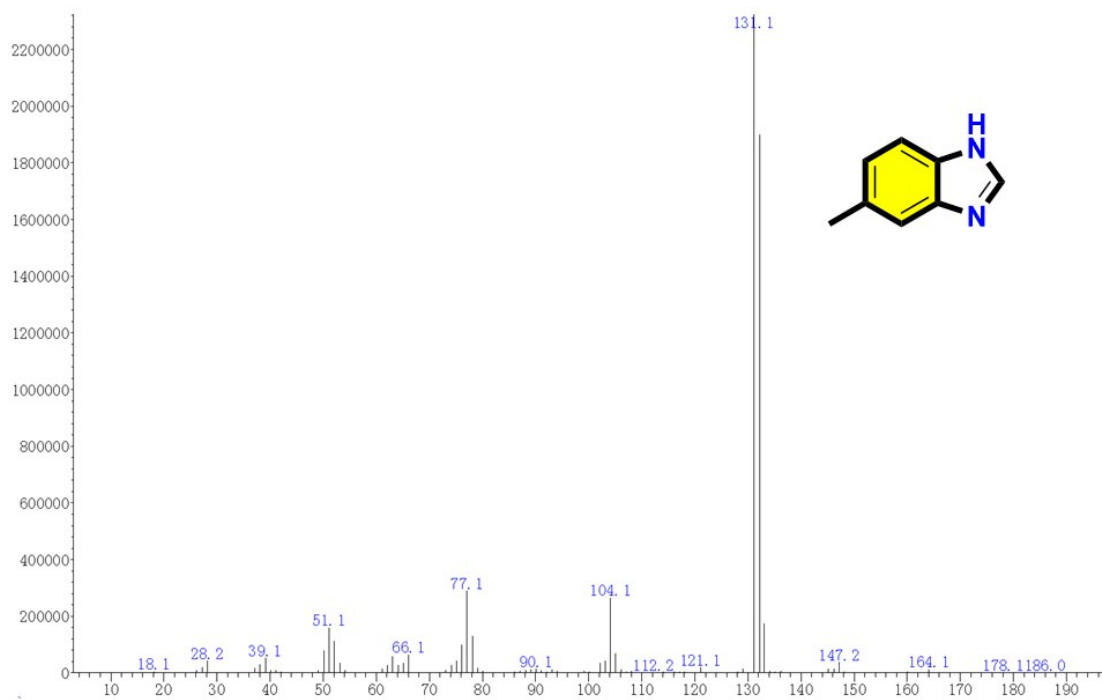**Figure S31.** The mass spectrum of **3j**.
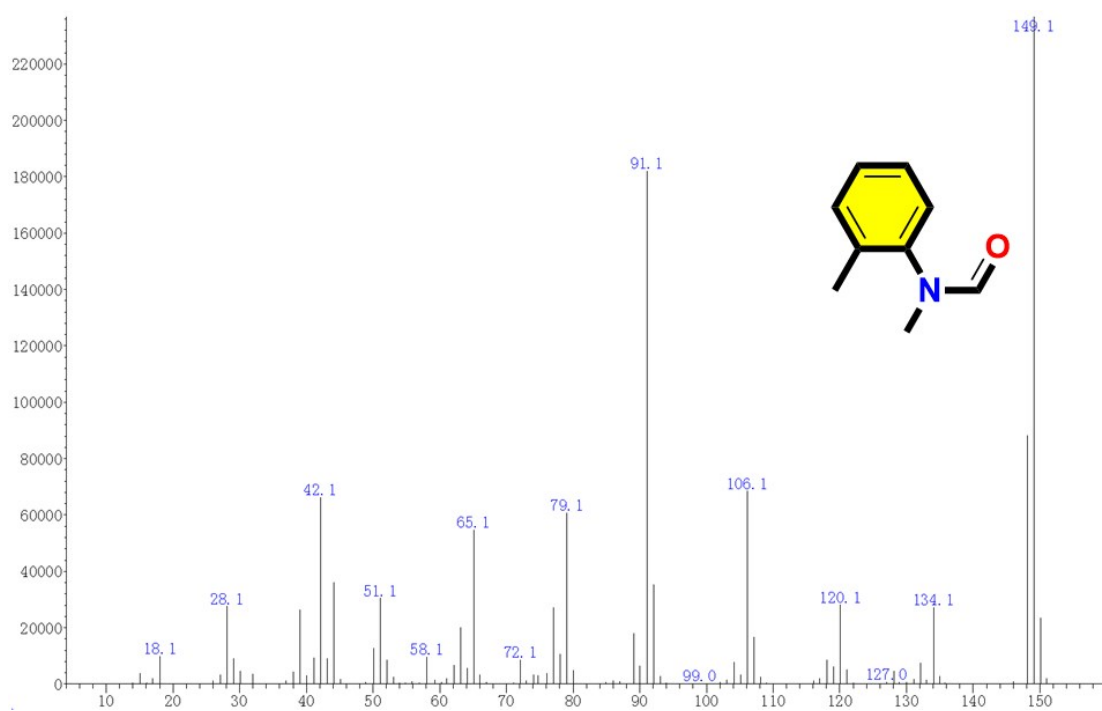
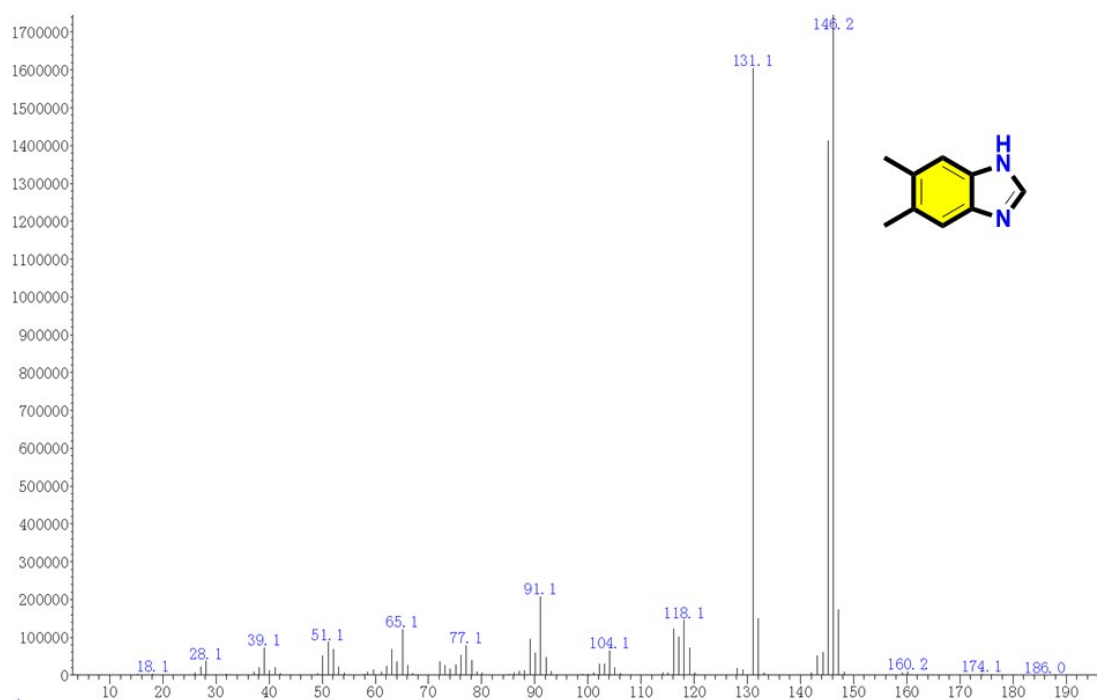**Figure S32.** The mass spectrum of **3k**.
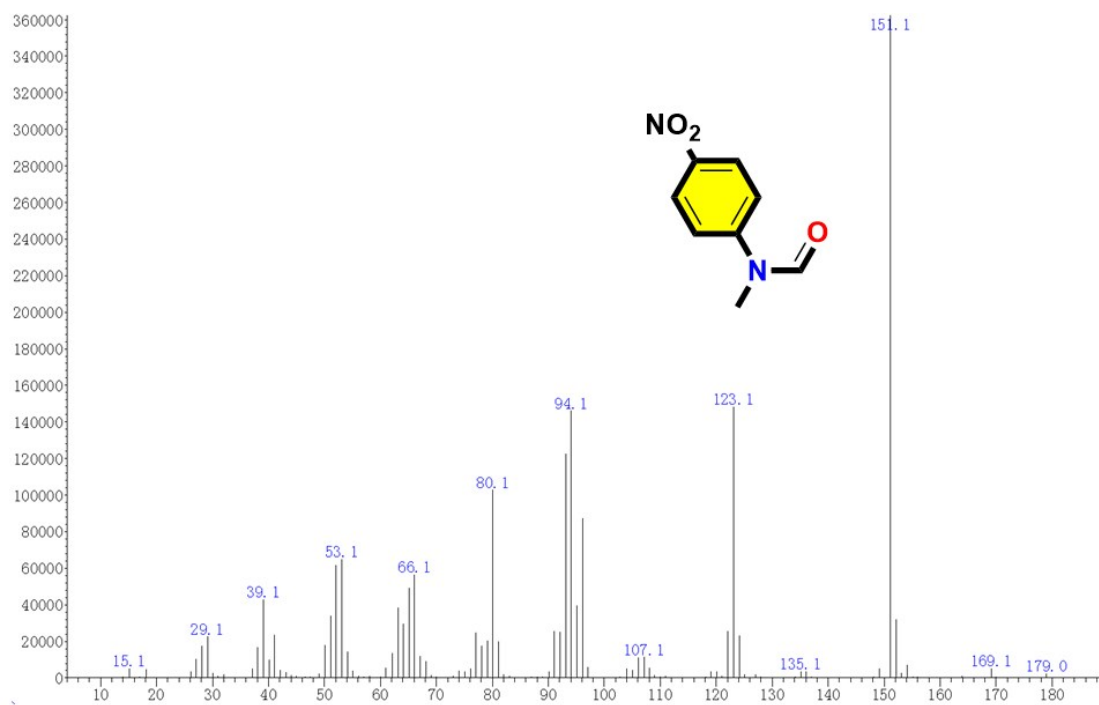
Figure S33. The mass spectrum of **3l**.
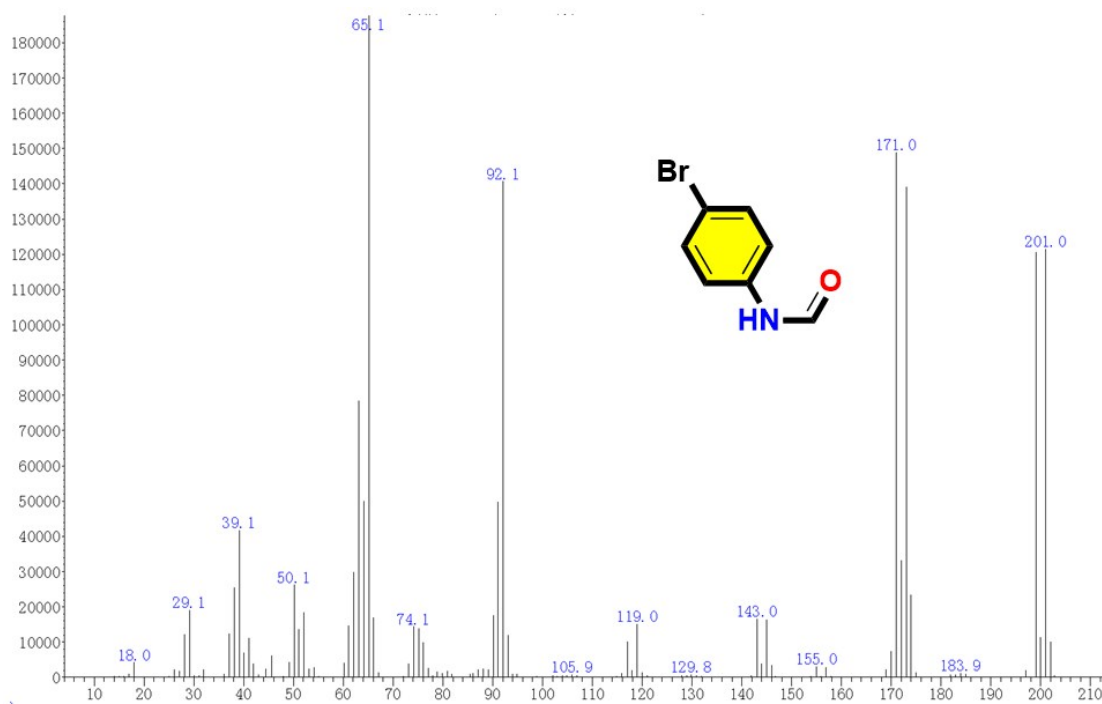
Figure S34. The mass spectrum of **3m**.
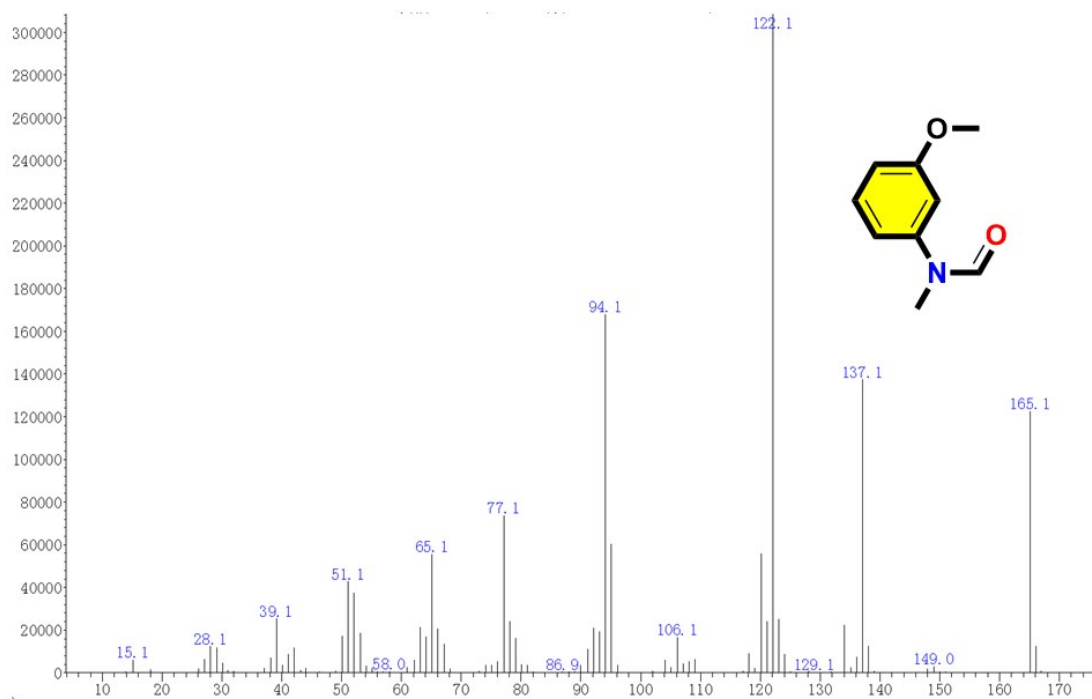
Figure S35. The mass spectrum of **3n**.
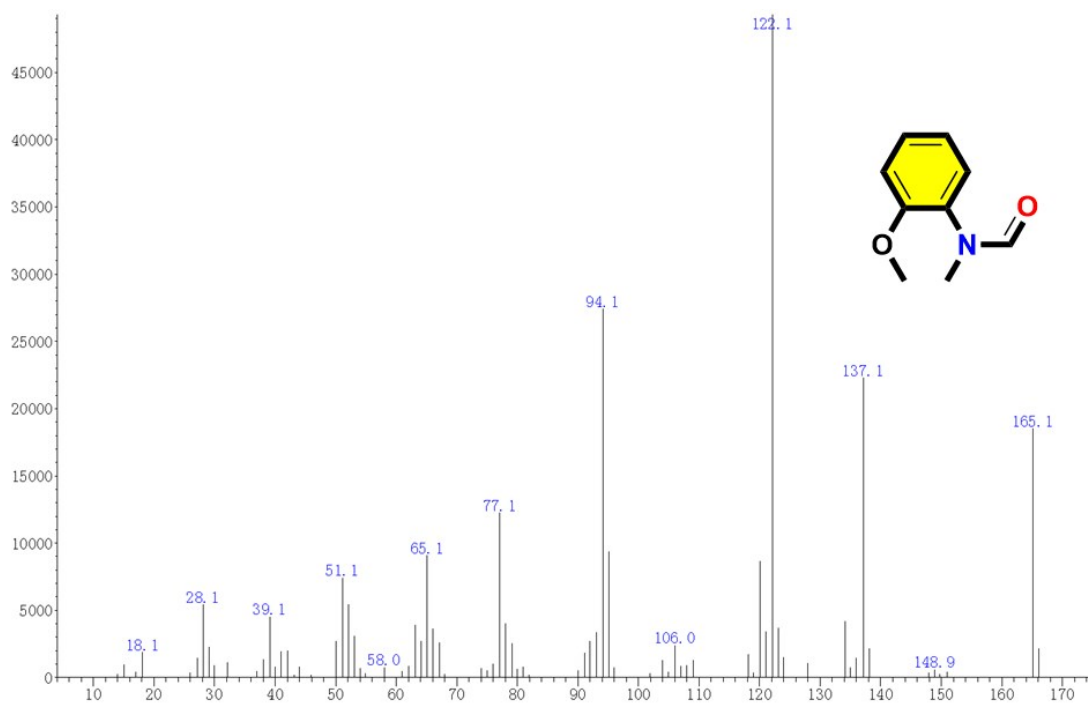
Figure S36. The mass spectrum of **3o**.
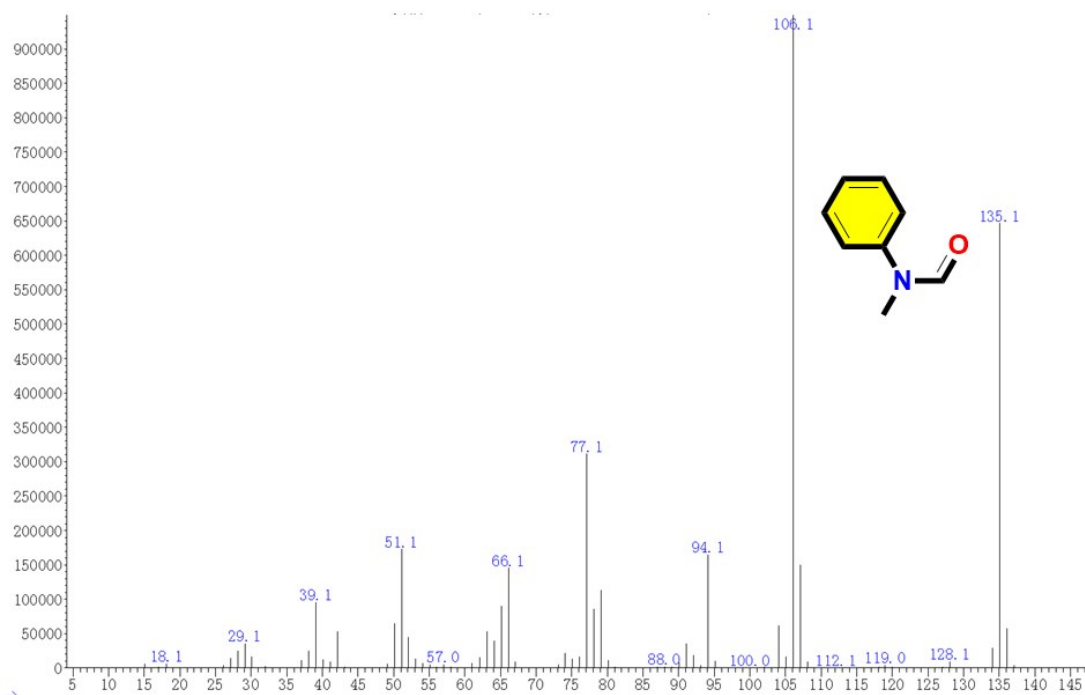
Figure S37. The mass spectrum of **3p**.

Figure S38. The mass spectrum of **3q**.

Figure S39. The mass spectrum of **3r**.

Figure S40. The mass spectrum of **3s**.
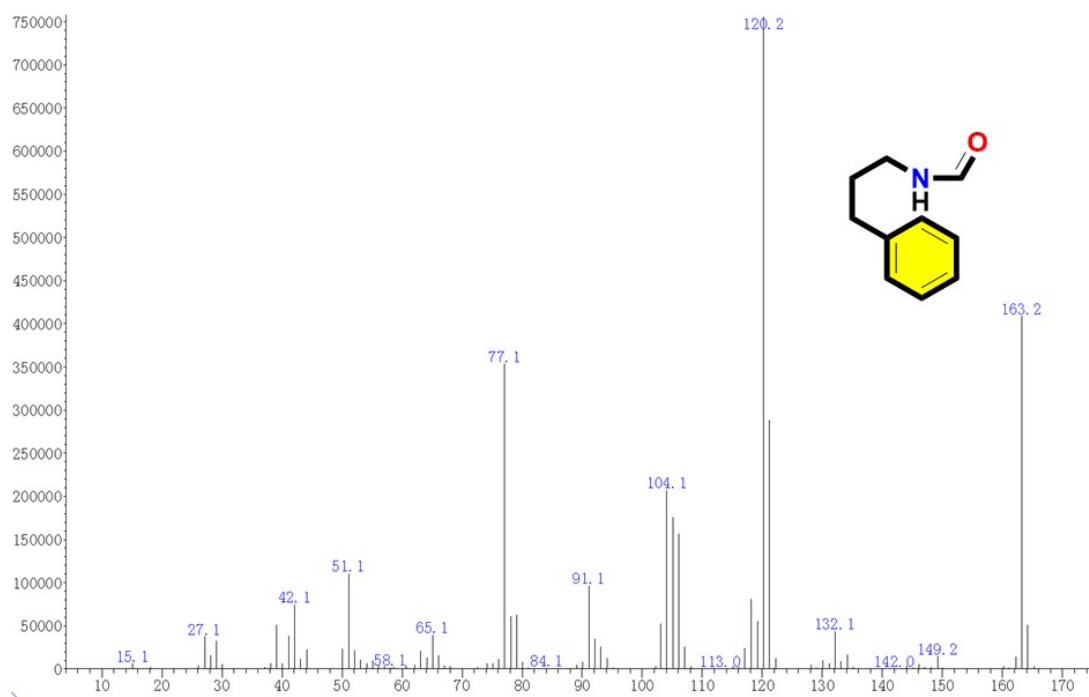
Figure S41. The mass spectrum of **3t**.

Figure S42. The mass spectrum of **3u**.

Figure S43. The mass spectrum of **3v**.

Figure S44. The mass spectrum of **3w**.

Figure S45. The mass spectrum of **4a**.
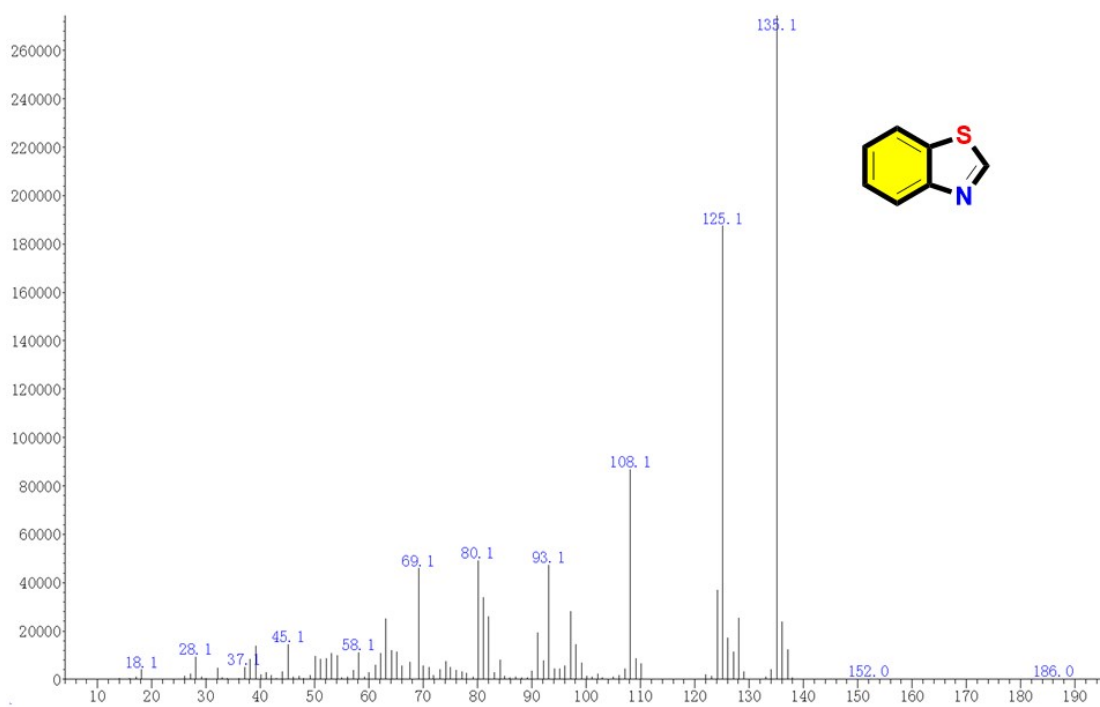

Figure S46. The mass spectrum of **4b**.

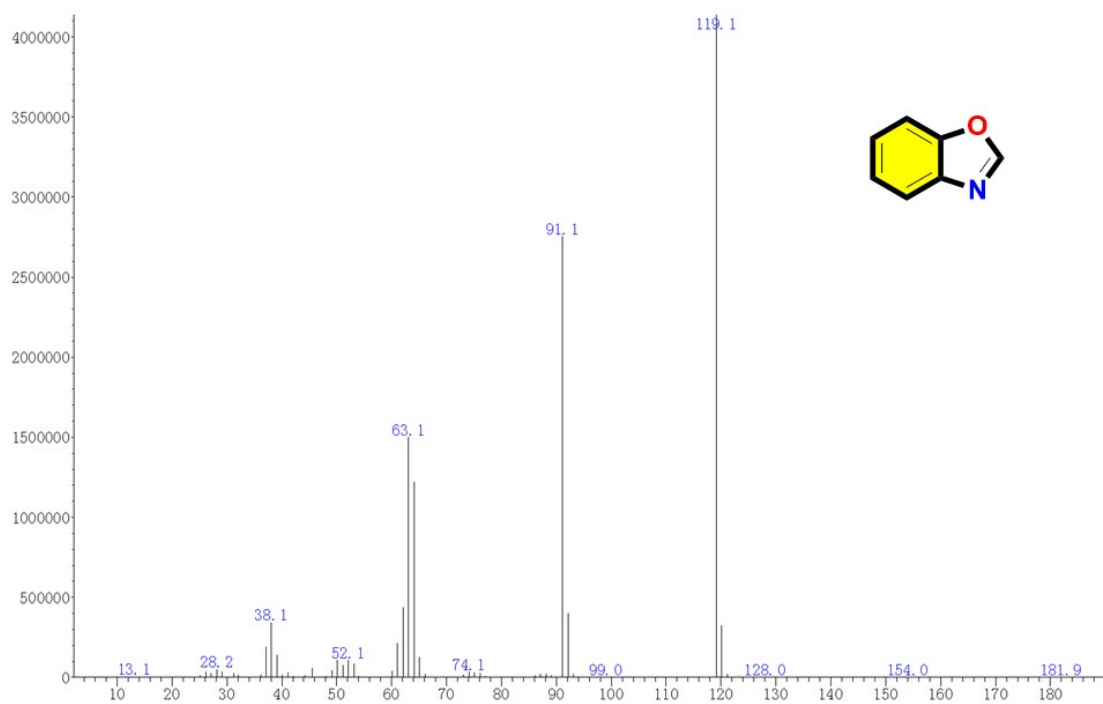**Figure S47.** The mass spectrum of **4c**.
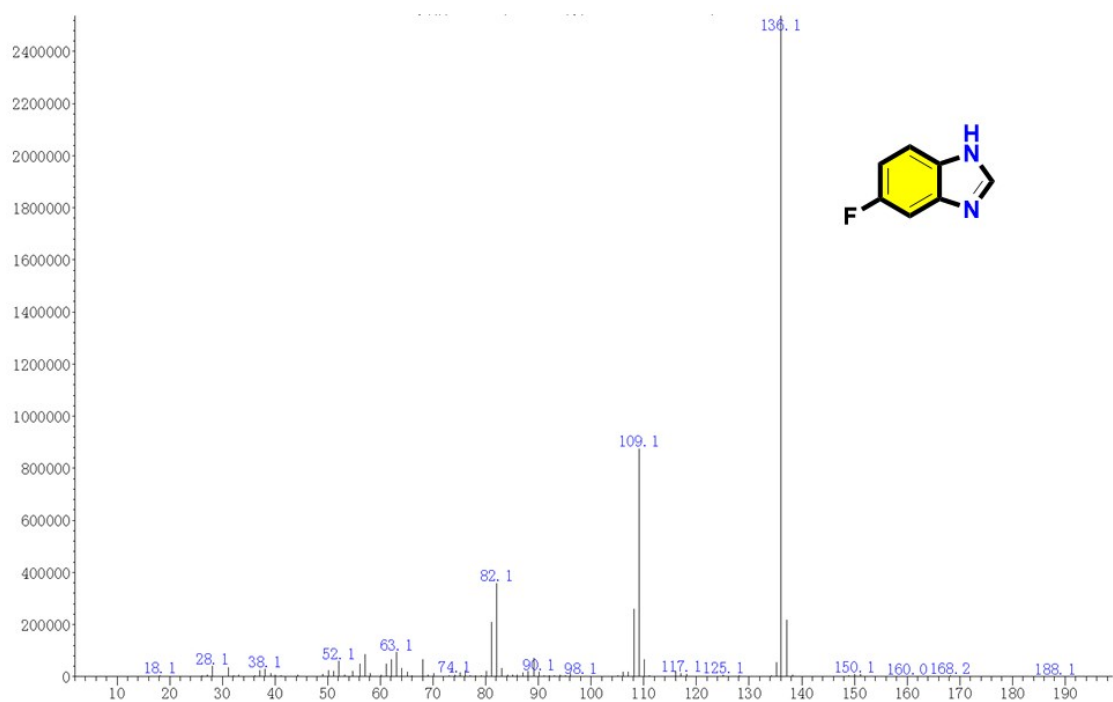

Figure S48. The mass spectrum of **4d**.

Figure S49. The mass spectrum of **4e**.

Figure S50. The mass spectrum of **4f**.

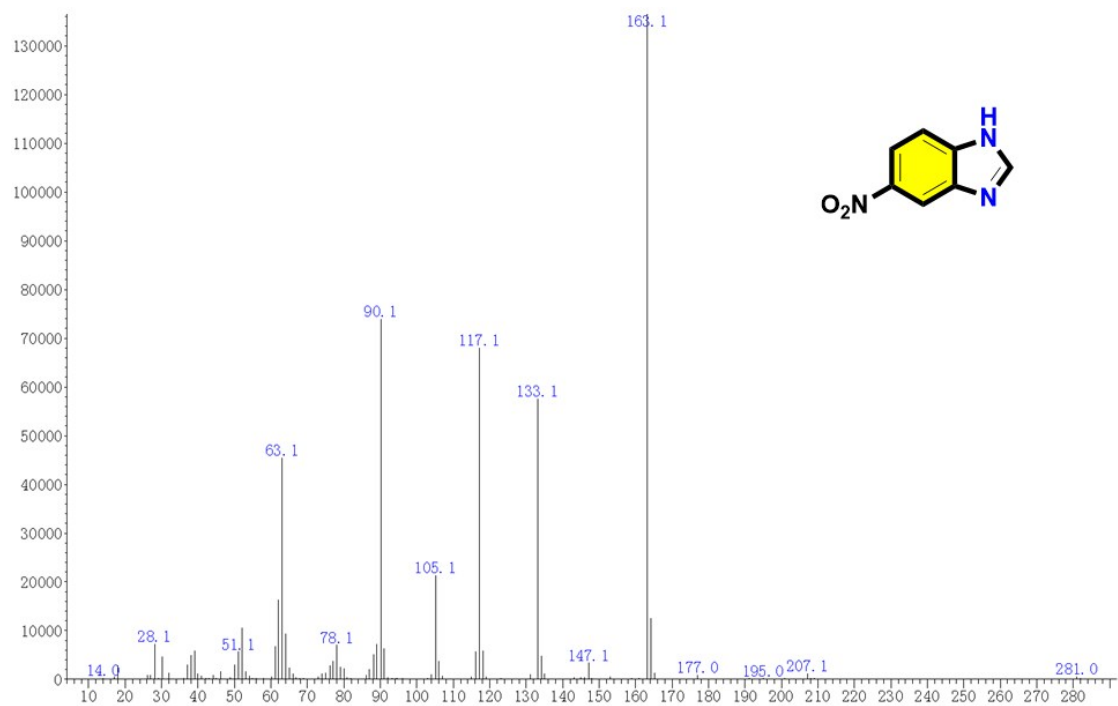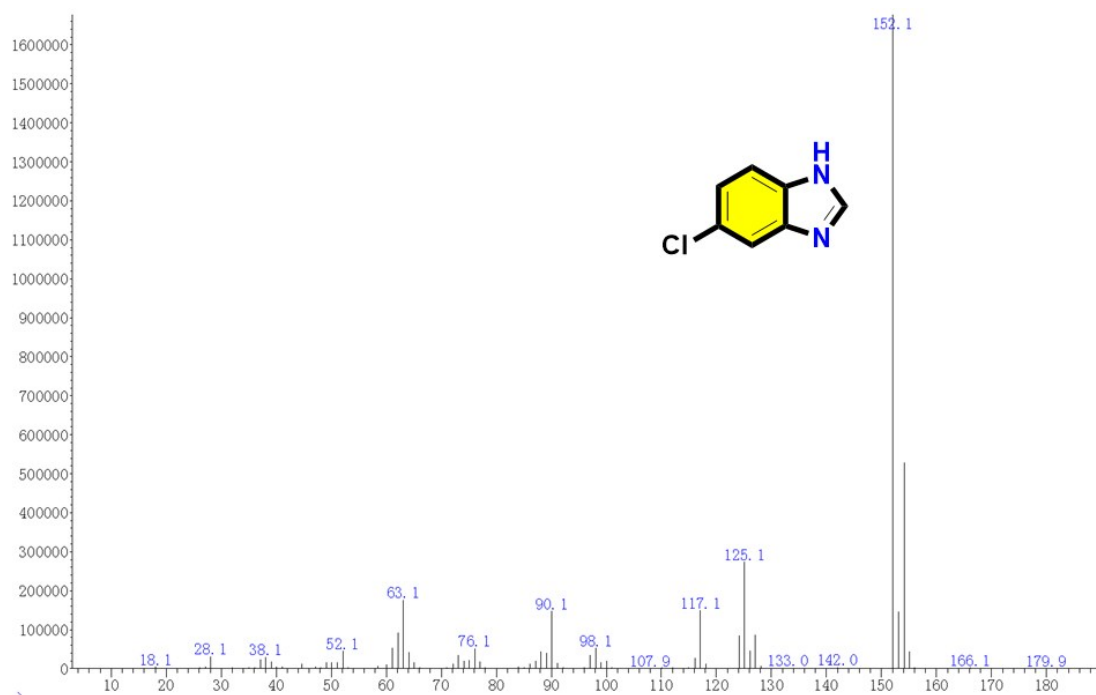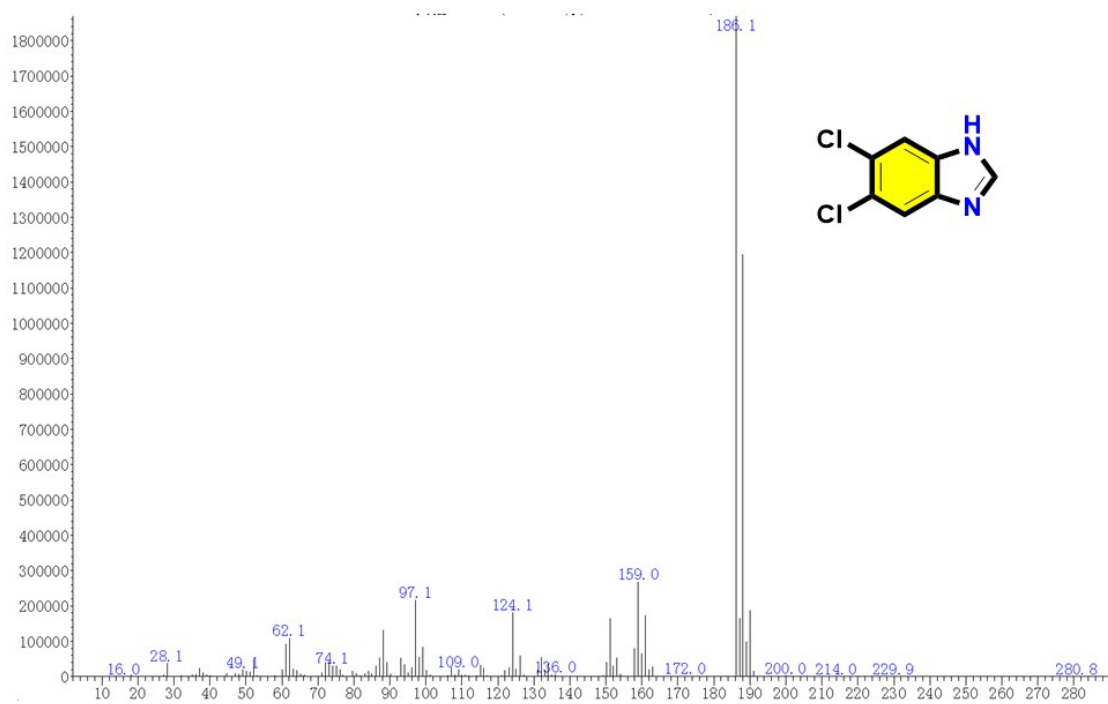**Figure S51.** The mass spectrum of **4g**.

Figure S52. The mass spectrum of **4h**.